

# **Molecular diagnosis of paleopathological human remains by using mass spectrometry**

**Ph.D. Thesis**

**Ágnes Bóna**

**Program leader: Prof. Balázs Sümegi, D.Sc.**

**Theme leader: Dr. László Márk, Ph.D.**



**Department of Biochemistry and Medical Chemistry**

**University of Pécs, Medical School**

**Hungary**

**2014**

# 1. Contents

<b>1. Contents</b>	2
<b>2. Abbreviations</b>	4
<b>3. Introduction</b>	6
3.1. Disease biomarkers in saliva	6
3.2. Tumor biomarkers	8
3.2.1. <i>Annexin protein family</i>	8
3.2.2. <i>BCL2 protein family</i>	10
3.2.3. <i>DJ1 protein</i>	11
3.2.4. <i>DLC1 protein</i>	12
3.2.5. <i>Heat shock proteins</i>	13
3.2.6. <i>S100 protein family</i>	14
3.2.7. <i>Vimentin</i>	15
3.3. Ancient evidence of osteosarcoma and tuberculosis	16
3.4. Biomarker investigation of paleopathological remains	18
3.5. Identification of proteins by mass spectrometry	20
3.5.1. <i>Proteomics</i>	20
3.5.2. <i>Protein separation by gel electrophoresis</i>	21
3.5.3. <i>General construction of a mass spectrometer</i>	23
3.5.4. <i>Matrix Assisted Laser Desorption/Ionization (MALDI)</i>	24
<b>4. Aims of the study</b>	30

<b>5. Materials and Methods</b>	31
5.1. Archaeological bone samples	31
5.1.1. <i>Osteosarcoma archaeological bone sample</i>	31
5.1.2. <i>Tuberculoid archaeological bone samples</i>	35
5.2. Extraction of ancient proteins	36
5.3. SDS-PAGE gel electrophoresis and enzymatic digestion	38
5.4. MALDI TOF/TOF MS-based identification of the ancient proteins	40
5.5. Statistical analysis	41
<b>6. Results and Discussion</b>	42
6.1. Osteogenic Sarcoma	42
6.2. Tuberculosis	48
<b>7. Conclusions</b>	52
<b>8. Acknowledgements</b>	54
<b>9. References</b>	55
<b>10. List of Publications</b>	76

## 2. Abbreviations

AD = Anno Domini

aDNA = ancient DNA

ANX = Annexin

BC = Before Christ

BCL2 = B-cell lymphoma 2-related protein

BP = Before Present

CHCA =  $\alpha$ -cyano-4-hydroxycinnamic acid

CID = Collision –Induced Dissociation

DHB = 2,5 dihydroxybenzoic acid

DLC-1 = Deleted in Liver Cancer 1

DTT = Dithiotreitol

EDTA = Ethylenediaminetetraacetic acid

HSP = Heat-Shock Protein

IAA = Iodoacetamide

LID = Laser Induced Decay

MALDI MS = Matrix Assisted Laser Desorption/Ionization Mass Spectrometry

MCP = Microchannel Plate detector

MTC = *Mycobacterium tuberculosis* Complex

PMF = Peptide Mass Fingerprint

PSD = Post Source Decay

RhoGAP = Rho GTPase-activating protein

R. T. = Room temperature

SA = Sinapinic acid

SDS PAGE = Sodium Dodecyl Sulphate Polyacrylamide Gel Electrophoresis

TFA = Trifluoroacetic acid

TOF = Time-of-Flight

VIM = Vimentin

Abbreviation of amino acids:

A = Alanine

C = Cysteine

D = Aspartate

E = Glutamate

F = Phenylalanine

G = Glycine

H = Histidine

I = Isoleucine

K = Lysine

L = Leucine

M = Methionine

N = Asparagine

P = Proline

Q = Glutamine

R = Arginine

S = Serine

T = Threonine

V = Valine

W = Tryptophan

Y = Tyrosine

## 3. Introduction

### 3.1. Disease biomarkers in saliva

Based on the previous work of our research group, tumor biomarker identification in saliva (Jarai et al., 2012), we started to analyse paleopathological bone samples to find potential biomarkers for two different ancient diseases. A cancerous disease, malignant bone tumor, osteosarcoma and an infectious disease, tuberculosis caused by *Mycobacterium tuberculosis* were analysed.

The analysis of human clinical body fluid samples, searching for disease biomarkers using proteomics is an important research field nowadays. Body fluids flow through the body and come in contact with several tissues of different organs picking up proteins. These proteins serve as possible biomarkers of disease and may provide new clues for drug development.

Oral cancer affects about 360,000 people worldwide (Hu et al., 2007). More than half of oral cancers are advanced by the time they are detected (Gonsalves et al., 2007; Weinberg and Estefan, 2002), due to the poor symptomatology for a long period. There is still no appropriate non-invasive, high-throughput diagnostic technique to develop the early signs of malignant transformation at least at those who are at a high risk. Early diagnosis plays a key role in disease progression, treatment response and ultimately, quality of life and patient survival (Marocchio et al., 2010).

Identifying protein-type biomarkers in body fluids collected at the clinic and analysed using mass spectrometry could solve the problem of the limited early detection of oral cancer (Szanto et al., 2012) as well as head and neck squamous carcinoma (Jarai et al., 2012).

Saliva is protein rich, and may constitute a valuable source of diagnostic and therapeutic markers in oral cancer patients (Drake et al., 2005; Edgar, 1992; Yao et al., 2003). Protein biomarkers derived from oral cancer cells have been identified after SDS-PAGE and tryptic digestion using MALDI TOF/TOF MS instrument by our research group. Comparing to healthy controls we found annexin 1 and 2 and

proteins such as peroxiredoxin1 and 2 and thioredoxin peroxidase in oral tumor patients (Szanto et al., 2012). Increased level of annexin 1, zinc finger protein 28, regulator G-protein 3, indoleamine 2,3-dioxygenase, OFD1 protein and CEP290 protein were found in the saliva samples of malignant cancer patients (Jarai et al., 2012). These proteins may serve as potential tumor markers in the future.

## 3.2. Tumor Biomarkers

Tumor biomarkers are proteins or genes which are naturally produced in cells but their overexpression or in case of genes increased activity indicate tumorous mutation generated by cancerous cells. These substances are found among others in blood, urine, saliva, tumor tissue and bone. At present there are more than 20 tumor markers in clinical use. The markers are mostly characteristic to the type of the cancer. Nevertheless the tumor marker alone is not acceptable to prove the presence of mutation, further tests and other measurements e.g. biopsy is needed, to set the diagnosis. The reasons are the following, not all of the patients produce elevated level of markers or the increased level of the crucial proteins not always indicates tumorous disease. In addition tumor markers have not been identified for every type of cancer.

### 3.2.1. Annexin protein family

The name of Annexins derived from the Greek *annex* meaning “bring/hold together” what points to their main functions binding to and possibly holding together membranes. ANXs are soluble, hydrophilic intracellular proteins that bind to negatively charged phospholipids in a  $\text{Ca}^{2+}$  dependent manner ( $\text{Ca}^{2+}$  / phospholipid binding proteins). The binding is reversible; ANXs can be liberated from the phospholipid matrix using chelating agents. The different members of this family have different  $\text{Ca}^{2+}$  sensitivity and phospholipid head group specificity (e.g.: phosphatidic acid, phosphatidylserine, phosphatidylinositol).  $\text{Ca}^{2+}$  dependent signal transduction pathways are involved in the regulation, growth and apoptosis of the cells (Gerke et al., 2002). Dysregulation of ANXs has been reported in numerous cancers, affecting proliferation, invasiveness, cancer-related signalling pathways assuming its crucial role in tumoral development and progression (Deng et al. 2012; Hata et. al., 2014; Kwon et al, 2013; Lin et al., 2012; Luo et al., 2013; Mogami et al., 2013; Sun et al., 2013; Zeng et al., 2013).

The family member, ANXA10 protein (Figure 1) is highly responsible for the cellular proliferation of oral squamous cell carcinoma (Shimizu et al., 2012). The elevated level of this protein corresponds to the stage of the tumor growth. However, decreased expression was observed in case of gastric (Kim et al., 2009; Kim et al., 2010) hepatocellular (Liu et al., 2002; Peng et al., 2005) and bladder carcinoma (Munksgaard et al., 2011), suggesting a tumor suppressing and apoptosis inducing property of ANXA10 protein.

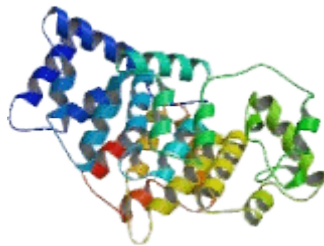


**Figure 1: 3D structure of ANXA10 protein (Length: 324 amino acids; 37.3 kDa)**  
([http://www.uscnk.com/directory/Annexin-A10\(ANX-A10\)-4780.htm](http://www.uscnk.com/directory/Annexin-A10(ANX-A10)-4780.htm))

### 3.2.2. BCL2 protein family

The B-cell leukemia/lymphoma-2 family proteins are encoded by BCL2 gene. The BCL2 protein family members all share sequence and structural similarity in their BCL2 homology (BH) domains. The BCL2 proteins have an important role in cell apoptosis. They can be divided into two subgroups according to their function: pro- and anti-apoptotic proteins. Apoptosis or programmed cell death can be triggered by cellular stress at the mitochondria (the intrinsic pathway). This pathway is responsible for the release of cytochrome c from the mitochondrial intermembrane space into cytosol, eventuating the formation of apoptosome and caspase-9 activation. The BCL2 proteins have important role in the regulation of this step (Ottina et al., 2012).

BCL2A1, B-cell lymphoma related protein A1 (Figure 2) has anti-apoptotic function during B-cell maturation. Overexpression of BCL2A1 indicates the presence of tumorous mutation including leukemia (Nagy et al., 2003), lymphoma (Mahadevan et al., 2005), stomach (Choi et al., 1995), breast cancer (Beverly et al., 2009), melanoma (Riker et al., 2008) and oral squamous cell carcinoma (Saleh et al., 2010). Increased level of BCL2A1 could be a possible reason for chemotherapeutic drug resistance. BCL2A1 proteins suppress apoptosis upon toxic insults and prevent cell death during chemotherapy. (Yajima et al., 2009)

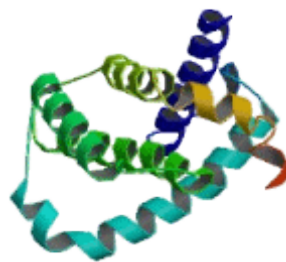


**Figure 2: 3D structure of BCL2A1 protein (Length: 175 amino acids; 20.3 kDa)**  
([http://www.uscnk.com/directory/BCL2-Related-Protein-A1\(BCL2A1\)-80252.htm](http://www.uscnk.com/directory/BCL2-Related-Protein-A1(BCL2A1)-80252.htm))

### 3.2.3. DJ1 protein

DJ1 protein (Figure 3) also known, as Parkinson disease (autosomal recessive, early onset) 7, PARK7 protein is encoded by DJ1 gene. DJ1 protein participates in transcriptional regulation, antioxidative stress reaction and in chaperone, protease and mitochondrial regulation. DJ1 has also a protecting role against oxidative stress induced cell death. The protein is located in the cytoplasm, nucleus and in the mitochondria of cells. DJ1 is secreted in almost all cells as well as in cancer cells and tissues. Significant level of DJ1 have been detected in squamous cell (Zhu et al., 2010), pancreatic (Tian et al., 2008), lung (Merikallio et al., 2012), renal cell carcinomas (Sitaram et al., 2009) and leukemia (Liu et al., 2008).

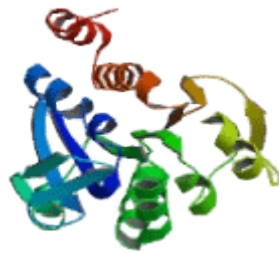


**Figure 3: 3D structure of DJ1 protein (Length: 187 amino acids; 19.9 kDa)**  
([http://www.uscnk.com/directory/Parkinson-Disease-7-Protein\(PARK7\)-80059.htm](http://www.uscnk.com/directory/Parkinson-Disease-7-Protein(PARK7)-80059.htm))

### 3.2.4. DLC1 protein

DLC1, deleted in liver cancer gene (Figure 4) encodes a Rho GTPase-activating protein (RhoGAP) DLC1, identified as a potent tumor suppressor (Kim et al., 2003; Plaumann et al., 2003; Yuan et al., 2004). DLC1 protein oncosuppressive effect is connected to its RhoGAP activity. The RhoGAP domain of DLC1 protein is able to enhance the GTPase activity of the RhoGTPase proteins promoting the hydrolysis of their bound GTP to GDP, rendering these proteins inactive. The different small GTPase members of RhoGAP family have a significant role in cell growth, morphogenesis, cell motility, cytokinesis, transformation and metastasis. These processes also involve oncogenic transformations and cancer progression (Guan et al., 2008; Kim et al., 2007). The down-regulation of DLC1 gene expression results the activation of Rho GTPases, the key mediators of oncogenesis (Peng et al., 2013; Qin et al., 2013). Reactivation of DLC1 gene in tumorous cells eventuate suppression in the proliferation and migration of cancer cells leading to apoptosis in vitro (Ullmannova-Benson et al., 2009). The down-regulation of DLC1 protein was found in melanoma (Sjoestroem et al., 2014), hepatocellular carcinoma (Wolosz et al., 2014) and in lung cancer (Kim et al., 2013) as well.

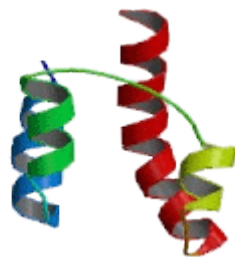


**Figure 4: 3D structure of DLC1 protein (Length: 1091 amino acids; 122.7 kDa)**  
([http://www.uscnk.com/directory/Deleted-In-Liver-Cancer-\(DLC1\)-6500.htm](http://www.uscnk.com/directory/Deleted-In-Liver-Cancer-(DLC1)-6500.htm))

### 3.2.5. Heat shock proteins

Heat shock proteins (Hsps) were first discovered when proteins were disordered by heat shock, oxidative stress or other protein-damaging events (Lindquist and Craig, 1988). They have a key role in the protection of malignant cells from spontaneous or therapy generated apoptosis. The elevated level of Hsps in various cancer types (Atkins et al., 2005; Kang et al., 2013; Kim et al., 2011; Li et al., 2012; Marinova et al., 2013) indicates the importance of these proteins in tumor progression and results chemoresistance. Hsps could shift the balance from denaturated state of protein toward functional protein. Hsps are molecular chaperons, which are able to modify the structures and interactions of other proteins. Hsp27, 70, 90, 110 are the most common expressed proteins after induced stress (Ciocca et al., 2005).



**Figure 5: 3D structure of Heat-shock protein beta-6**

**(Length: 160 amino acids; 17.1 kDa)**

**([http://www.uscnk.com/directory/Heat-Shock-Protein-B6-Alpha-Crystallin-Related\(HSPB6\)-5358.htm](http://www.uscnk.com/directory/Heat-Shock-Protein-B6-Alpha-Crystallin-Related(HSPB6)-5358.htm))**

### 3.2.6. S100 protein family

The S100 family contains 20 small acidic proteins containing calcium-binding EF-hand motifs. EF-hand motifs consist of two helices (E and F) joined by a loop, this loop is responsible for the binding of  $\text{Ca}^{2+}$ . One of the EF hands is on the C-terminal portion the other one is located at the N-terminus (specific to this protein family). S100 proteins show different cell-specific and tissue-specific patterns, which result their distinct functions in specific tissues or cell types. The members of this family take part in a variety of biochemical activities such as protein phosphorylation, enzyme activities,  $\text{Ca}^{2+}$  homeostasis, inflammation, cell proliferation and differentiation. S100 family proteins have significant role in tumorigenesis and metastasis. Some members of the family act as tumor promoters and others act as tumor suppressors (Salama et al., 2008).

Calgizzarin or S100A11 protein (Figure 6) has an important biological role in cell proliferation and differentiation. According to previous studies Calgizzarin is involved in tumor development and immortalization. Overexpression of Calgizzarin is seen in many cancers including colorectal (F Lam et al., 2010; Tanaka et al, 1995; Wang et al, 2008), gastric (Li et al., 2011; Mori et al., 2004; Oue et al., 2004), pancreatic (Chen et al., 2009; Ji et al., 2014; Ohuchida et al., 2006; Xiao et al., 2012), breast (Cross et al., 2005; Liu et al., 2010; McKiernan et al., 2011), prostate (Rehman et al., 2004), lung (Hao et al. 2012; Tian et al., 2007), bladder (Yao et al., 2007) and squamous cell carcinoma (Roesch-Ely et al., 2007; Wang et al, 2013).

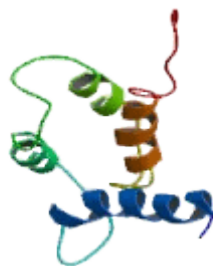


**Figure 6: 3D structure of Calgizzarin (Length: 105 amino acids; 11.7 kDa)**  
([http://www.uscnk.com/directory/S100-calcium-binding-protein-A11\(S100A11-S100C\)-0568.htm](http://www.uscnk.com/directory/S100-calcium-binding-protein-A11(S100A11-S100C)-0568.htm))

### 3.2.7. Vimentin

Vimentin or VIM (Figure 7) is a notable member of the intermediate filament family of proteins; it is expressed in normal mesenchymal cells. VIM is responsible for maintenance of cellular integrity and provides resistance against stress. Furthermore VIM has been identified as a marker for several tumorigenic events related epithelial-mesenchymal transition (EMT). Elevated level of VIM is associated with numerous epithelial cancers, including prostate cancer (Rodrigues et al., 2011; Singh et al., 2003; Wei et al., 2008), gastrointestinal tumors (Hou et al., 2012; Noguchi et al., 2002), tumors of the central nervous system (Satelli and Li, 2011), breast cancer (Bocca et al., 2014; Deng et al., 2013; Lehtinen et al., 2013), malignant melanoma (Fink-Puches and Smolle, 1993; Hendrix et al., 1996) and lung cancer (Feng et al., 2012; Giarnieri et al., 2013; Tauler et al, 2010). Also because of its overexpression in different tumorous cells, participation in the growth, invasion and migration of the tumorous cells, VIM can be used as a target to deliver therapeutic agents to the tumor site (Zamay et al, 2014).



**Figure 7: 3D structure of VIM protein (Length: 466 amino acids; 53.6 kDa)**  
([http://www.uscnk.com/directory/Vimentin\(VIM\)-1040.htm](http://www.uscnk.com/directory/Vimentin(VIM)-1040.htm))

### 3.3. Ancient evidence of osteosarcoma and tuberculosis

Osteosarcoma is the most common primary bone tumor characterized by the production of osteoid matrix from malignant cells derived from progenitor cells in the osteoblast lineage. It typically occurs in the long bones of the near metaphyseal growth plates of children and young adolescents (Beckingsale and Gerrand, 2010). These mesenchymal tumor related mutations escape from the cells leading to excessive proliferation without differentiation from normal osteoblastic cells during the cell cycle. This highly aggressive neoplasm frequently metastasizes in the lungs. After an initial diagnosis, patients usually receive standard treatment such as neoadjuvant chemotherapy and surgical resection.

Osteosarcoma has a poor prognosis because metastases are usually developed prior to clinical diagnosis. Despite intensive research for new therapies, the survival rate for patients with advanced disease still remains low.

The earliest known case affected a male Celt (ca. 800–600 BC) from Switzerland with a possible osteosarcoma or chondrosarcoma (Brothwell, 1967). A possible osteosarcoma of the pelvis has been noted in a young individual from Ancient Egypt, dating to about 250 AD (Ruffer and Willmore, 1914), and a well-documented case of osteosarcoma, with the typical radiographic “sunburst” pattern, has been reported in the femur of a native Peruvian dating to 800 BP (Aufderheide et al., 1997). Additional cases of osteosarcoma have been observed in a young female femur from the prehistoric population of Oahu in Hawaii (Suzuki, 1987), and in a zygomatic bone from the French Middle Ages (Dastugue, 1965) in a case of 17th century mandible from West Virginia (Kelln et al. 1967). Possible osteosarcomas have been detected in a young male from the Saxon necropolis of Standlake, England (Brothwell, 1981) and in medieval skulls from the Czech Republic (Strouhal et al., 1996) and France (Blondiaux, 1986). Probable cranial hemangiosarcoma has been documented in an elderly female from Italy, 3rd Century BC (Capasso et al., 1992) and in a humerus from Peru, 12–14th Centuries AD (Aufderheide et al., 1997) and a possible Ewing’s sarcoma in a juvenile skull from Bronze Age of Tartaren, Spain (Campillo, 1976). Only a few cases of neoplasms have been documented in Central and South American mummies, for example a rhabdomyosarcoma (4–7th Centuries AD) in 2 children from Chile (Gerszten and Allison, 1991).

Tuberculosis is a chronic infectious disease, caused by bacteria of the *Mycobacterium tuberculosis* complex (MTC), including *Mycobacterium tuberculosis* and *Mycobacterium bovis* being the most common cause of illness in humans. Tuberculosis, one of the oldest recorded human afflictions, is still one of the most deadly and common major infectious disease today, despite the worldwide use of a live attenuated vaccine and several antibiotics (Kinsella et al., 2003; Mathema et al., 2006; Smith, 2003; Stone et al., 2009). The most common symptoms are chronic cough with blood-tinged sputum, fever and weight loss (phthisis). Tuberculosis could infect the lymph nodes in the neck, armpits and groin forming large, swollen lumps known as scrofula. The infection is spread through the air with coughing and sneezing. It infects approximately one-third of the world's population, although the vast majority of these potential cases are in Africa or Asia.

*Mycobacterium tuberculosis* complex could be very old. The first evidence of the existence of *Mycobacterium* infection is represented by an extinct bison dated 17,000 years BC (Rotschild et al., 2001). The excavation of human skeletal remains can confirm evidence of infection as a proportion of chronic cases will have bony lesions. The most characteristic parts of the skeleton involved are the spine, hip and knee joints, the hands and the feet, but any bone can be involved. Typical lesions are destructive with some bone regeneration during healing. This may result in collapse of vertebral bodies causing angulation of the spine (kyphosis), ankyloses of joints and cavity formation in any bone. The presence of the disease was detected in an 5400-year-old Predynastic Egyptian human skeleton (Crubezy et al., 1998) and in ancient remains from the end of Predynastic time, from around 3000 BC (Zink et al., 2001). Further, precolumbian presence of the disease was found in Chile (Arriaza et al., 1995). European evidences of tuberculosis are from Dorset, England (400-230 BC) (Mays and Taylor, 2003) and from Lithuania (Faerman and Jankauskas, 2000) both from the Iron Age. Researchers have found the medieval presence of tuberculosis in England (Mays et al., 2001; Taylor et al., 1999) and in Hungary as well (Haas et al., 2000a).

### 3.4. Biomarker investigation of ancient remains

Recent advances in bioanalytical techniques especially in modern mass spectrometry (MS) have made the possibility to obtain sequence information from subpicomolar quantities of fragmented ancient proteins and peptides (Asara et al., 2007; Boros-Major et al., 2011; Buckley et al., 2008a, 2008b, 2009, 2010; Cappellini et al., 2012; Nielsen-Marsh et al., 2005, 2009; Orlando et al., 2013; Ostrom et al., 2006).

Certain proteins, which are characteristic for tumorous disease can be extracted from the diseased cells, were presumably transported earlier by the blood and absorbed to the bone hydroxyapatite (Schultz et al., 2007). Diagnosis of cancer as well as osteogenic sarcomas from ancient human skeletal remains is not an easy task by using classic morphological methods. Therefore a biomolecular approach to diagnosis in addition to osteological examination can be beneficial (Schultz et al., 2007). Recently, proteomic profiling of human tumors has provided a better understanding of the molecular pathogenesis of neoplastic diseases and has identified novel biomarkers for early diagnosis. SELDI-TOF-MS (Surface Enhanced Laser Desorption/Ionization Time of Flight Mass Spectrometry) and protein microarray high throughput analysis enable to detect biomarkers from the serum samples of osteosarcoma patients (Li et al., 2009). Based on the MALDI-TOF MS analysis of clinical benign bone tumor and malignant osteosarcoma several biomarkers are up- or down-regulated (Li et al., 2010). Also MALDI-TOF MS analysis of human osteosarcoma MG-63 cells showed the alterations of some genes and proteins (Zhao et al., 2006).

*Mycobacterium tuberculosis* has the property to disseminate in the body via the blood and lymphatic systems and replicate in bones, leaving characteristic lesions in it. These facts make the paleopathological/paleoepidemiological research of tuberculosis particularly timely. Unfortunately, there are several biases of the classical osteoarcheological studies of MTC, such as the differentiation between the taphonomic and paleopathologic conditions of the examined series, the problematic of the diagnostic criteria (Palfi and Molnar, 2009).

A biomolecular approach to diagnosis is probably more reliable than gross osteological examination of archaeological skeletal remains. The survive of pathological biomarkers in ancient skeletal remains is a major prerequisite for any molecular analysis and is thus essential for the pathological examination of archaeological bones. The use of DNA techniques to detect pathogenic agents in archaeological remains has exponentially increased recently. Numerous papers include detection of aDNA for tuberculosis (Crubézy et al., 2006; Donoghue et al., 2005; 2009; 2010; Gernaey et al., 2001; Haas et al., 1999; Hershkovitz et al., 2008; Taylor et al., 2007), leprosy (Haas et al., 2000b; Montiel et al., 2003; Rafi et al., 1994; Taylor et al., 2000; 2009), malaria (Sallares and Gomzi, 2001; Taylor et al., 1997), plague (Drancourt et al., 1998; Raoult et al., 2000) and syphilis (Kolman et al., 1999). However, many of these studies have been criticised and doubts have been cast authenticity of their results (Kolman and Tuross, 2000; Montiel et al., 2003; Wilbur et al., 2009).

However the analysis of *M. tuberculosis* is more reliable investigation method compared to the analysis of other possible biomarker for tuberculosis such as mycolic acid (Mark et al., 2010). Mycolic acids are long-chain fatty acids (up to 90 carbon atoms); these molecules are components of the mycobacterial cell envelope. In case of mycolic acids, clinical protocols and standards cannot directly be used for paleopathological samples (Minnikin et al., 2010) due to the chemical and biochemical processes e.g. amidation, carbamidomethylation, ester formation, fragmentation etc. taking place during hundreds of years. Another identification problem is that mycolic acid standards (Sigma-Aldrich) are not reproducible and do not correlate always with the authentic material (Mark et al., 2011). Only in cases where the mycolate profiles closely mirror those of modern standards of mycobacterial disease can be diagnosed with high confidence level.

## **3.5. Identification of proteins by mass spectrometry**

### **3.5.1. Proteomics**

The term „proteome” originates from the words protein and genome. It includes all of the proteins encoded by the genome in an organism. The genome of an organism is always static contrarily to its proteome, which is changing dynamic to one cell type to another and keeps changing even at different activity and development stages of the same cell type.

Proteomics deals with the identification, quantity, structure, function, localization, modifications and interaction of proteins. Proteins are major constituents of muscle, cartilage and bones. Proteins have various crucial functions, some of them serve as a catalyst for several biochemical reactions (e.g. enzymes), act as a transmitter (e.g. neurotransmitters), regulate cell reproduction, influence the growth and development of various tissues (e.g. trophic factors), participate in the transport of vital molecules (e.g. haemoglobin) or defend the body against disease (e.g. antibodies). Missing or defective proteins are the cause of many diseases and therefore serve as diagnostic indicators (biomarkers) and can help in drug development. The change in the proteome reflects also the differential activity of genes dependent on the cell type to express the protein needed for the particular function.

Furthermore, the protein profile of the cell can vary depending on the different modification of the protein such as acetylation, phosphorylation and glycosylation. These posttranslational modifications alter the functions of proteins.

Unequalled sensitivity, detection limits, speed and diversity of its applications made mass spectrometry an excellent tool for proteomic investigations.

### 3.5.2. Protein separation by gel electrophoresis

SDS-PAGE is the most commonly practised gel electrophoresis technique used for proteins. Electrophoresis is based on the migration of charged proteins in an electric field. The speed of migration depends on the charge, shape and size of the protein. Electrophoretic separations are generally carried out in gels made up of chemically inert, polymerization product of acrylamide. The polyacrylamide gel acts as a molecular sieve, the proteins migrate in proportion to their charge-to-mass ratio (Figure 8).

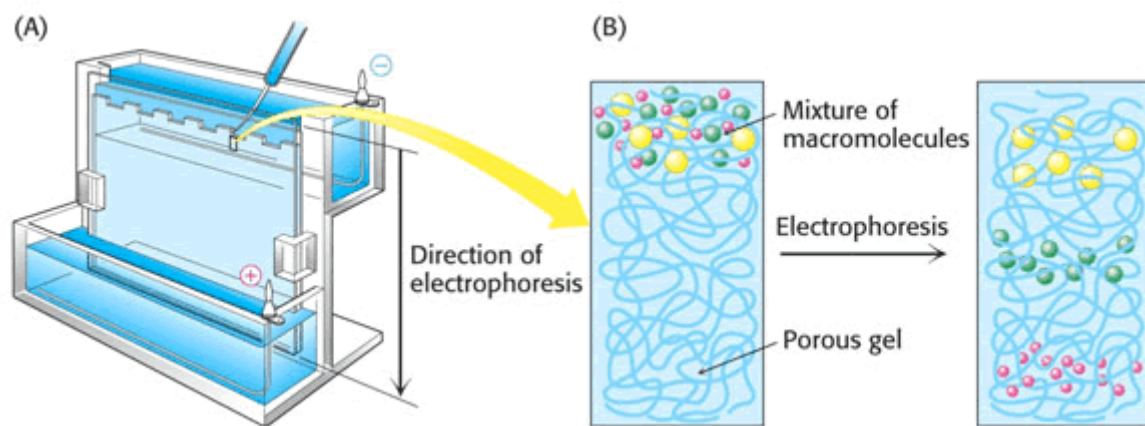


**Figure 8: Sample loading (A) and the separation of macromolecules in gel electrophoresis (B)**

([http://elte.prompt.hu/sites/default/files/tananyagok/practical\\_biochemistry/ch07s03.html](http://elte.prompt.hu/sites/default/files/tananyagok/practical_biochemistry/ch07s03.html))

The proteins are first dissolved in SDS (sodium dodecyl sulphate) solution. SDS is an anionic detergent that disrupts the noncovalent interactions in native proteins. SDS divides hydrogen bonds, blocks hydrophobic interactions and substantially unfolds the protein molecules, eliminating the secondary and tertiary structures. SDS gives a complex with the denatured protein, the complex is negatively charged. The net negative charge depends on the mass of the protein, because one molecule of SDS is connected to two amino acid residues. The negative charge of the complex is much greater than the charge on the native protein; this

native charge is thus rendered insignificant. DTT (dithiothreitol) is also added to the protein sample to reduce disulphide bonds between cysteine residues.

The protein samples are loaded into the gel pockets using Hamilton syringe. The electrical current in an electrophoresis cell is mainly transmitted by the ions supplied by buffer compounds; proteins contain only a small portion of current carrying ions. Moreover the buffers maintain the desired pH, and provide a medium for heat dissipation.

After electrophoresis, the proteins in the gel are visualized by adding a dye such as Coomassie Brilliant Blue. The detection limit of this staining method is 0.1  $\mu\text{g}$  (~2 pmol). The mobility of the polypeptide chains is linearly proportional to the logarithm of their mass. The position of an unidentified protein is compared with the positions of proteins of known molecular weight migrate in the gel (molecular weight standard). For the digestion of the excised gel bands a proteolytic enzyme such as trypsin is used. Trypsin cleaves after arginine and lysine residues (Olsen et al., 2004) except if they are followed by proline.

### 3.5.3. General construction of a mass spectrometer

The basic functions of a mass spectrometer are: the production of gas-phase ions from sample molecules (in the ion source), the separation of the ions according to their mass-to-charge ratio ( $m/z$ ) (in the analyser) and the detection of the separated ions. Mass spectrometers consist of three main parts: an ion source, a mass analyser and a detector (Figure 9). The instrument requires high vacuum ( $10^{-4}$ - $10^{-7}$  mbar) provided by a roughing and a turbomolecular pump in two steps. The ions produced in the ion source have to go through the mass spectrometer without hitting air molecules, because collisions could neutralize the charge of the ions or change the path of the ions leading to the loss of sensitivity and reproducibility.

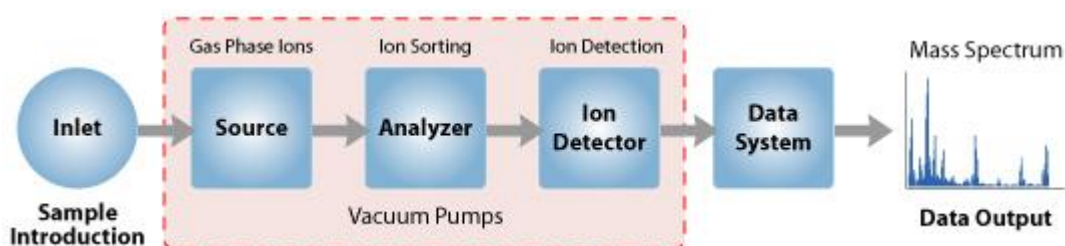


**Figure 9: Schematic representation of a mass spectrometer.**

([http://www.premierbiosoft.com/tech\\_notes/mass-spectrometry.html](http://www.premierbiosoft.com/tech_notes/mass-spectrometry.html))

For the ionization of gas phase analyte ions two methods are used. Positive ionization mode means generally the addition of an  $H^+$  ion; negative ionization mode is achieved mostly by the removal of an  $H^+$  ion. Proteins and peptides are usually analysed in positive ionization mode, because the  $NH_2$  group of the proteins readily accepts  $H^+$  ion. The most commonly used soft ionization methods are electrospray ionization (ESI) and Matrix Assisted Laser Desorption/Ionization (MALDI). The most often used analysers are time-of-flight (TOF), ion trap (IT) and quadrupole-time-of-flight (Q-TOF) analysers. The ion intensity at different  $m/z$  values is recorded normally at an electron multiplier type detector.

### 3.5.4. Matrix Assisted Laser Desorption/Ionization (MALDI)

Matrix Assisted Laser Desorption/Ionization (MALDI) is an ideal tool for the analysis of high molecular weight, non-volatile biopolymers, especially proteins and peptides. MALDI soft ionization method was developed at the University of Munster, Germany by Franz Hillenkamp and Michael Karas (Hillenkamp et al., 1990; Karas et al., 1987; Karas and Hillenkamp, 1988) simultaneously with Koichi Tanaka, Shimadzu Research Laboratories, Kyoto, Japan (Tanaka et al., 1988). While Tanaka used finely dispersed metal powder in a glycerol matrix for ionization upon irradiation by a pulsed UV laser, Hillenkamp worked with organic matrix to facilitate ionization and desorption of the sample for the same purpose.

MALDI matrices are aromatic, UV light (energy) absorbing molecules dissolved in a volatile and acidic solution. The matrix plays a key role in the absorption of the laser light energy and causing the analyte to vaporize. It also serves as a proton donor or acceptor ionizing the analyte either in positive or in negative ionization mode. The matrix is usually mixed with the sample on a target plate; this is the widely used dried droplet method. The solvent is evaporated before the sample is introduced into high vacuum by laser ablation. The most popular, frequently used matrices in proteomics are:  $\alpha$ -cyano-4-hydroxycinnamic acid (CHCA), 2,5 dihydroxybenzoic acid (DHB) and sinapinic acid (SA) (Figure 10).

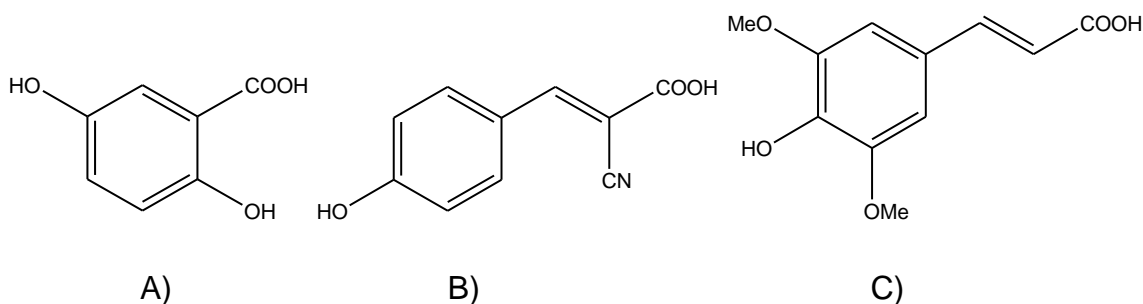


**Figure 10: Widespread used MALDI matrices: A) DHB, B) CHCA, C) SA**

MALDI MS instrument generally equipped with time-of-flight (TOF) analyser, first published in 1946 by Stephens (Stephens, 1946). The pulse of nitrogen laser ( $\lambda=337\text{nm}$ ) is focused onto the sample-matrix spot initiating ionization and desorption/ablation. Due to the extremely short laser shots the analyte avoids thermal degradation, longer irradiation cause only the heating of the bulk material. The ions formed are accelerated to the same kinetic energy. In a field-free drift tube they are separated in time according to their different  $m/z$  values, lighter ions reach the detector earlier than the heavier ones. The detector is usually a microchannel plate (MCP) detector which converts the ions to electrons; the whole process is based on the multiplication of electrons via secondary emission in order to increase the signal intensity of the detected ions. Single-shot spectra show a low signal-to-noise ratio, therefore 500-1000 single-shot spectra are usually accumulated to produce the final spectrum. MALDI has a large tolerance to contamination by salts, buffers and detergents (Chen et al., 1998; Stump et al., 2002).

Typical MALDI spectra include mainly the monocharged molecular species by protonation in positive ionization mode, deprotonated compounds are usually detected in negative ionization mode. The instrumental setup where the ions are travelling on a straight line from the point of their creation to the detector is called linear TOF. The resolution is limited because laser-desorbed ions possess large initial kinetic energy which is superimposed to their kinetic energy during the acceleration process. Higher acceleration voltage results higher resolution.

The reflectron/reflector has been developed by Mamyrin and coworkers in St. Petersburg (Mamyrin et al., 1973). The reflectron acts as an ion mirror that allows of the ions to penetrate the reflectron until they reach zero kinetic energy. A reflectron generally consists of a retarding electric field located behind the field-free region opposed to the ion source (Figure 11). The kinetic energy of the leaving ions remains unaffected; the time-of-flight depends only on the  $m/z$  of the ion, how deep the ion penetrates into the reflecting field. The more energetic ions will fly deeper into the electric field, therefore, have a longer flight path. The correction in initial kinetic energy provides higher resolution. MALDI TOF/TOF tandem mass spectrometers apply linear TOF as the first mass analyser and a reflectron TOF as the second mass analyser.

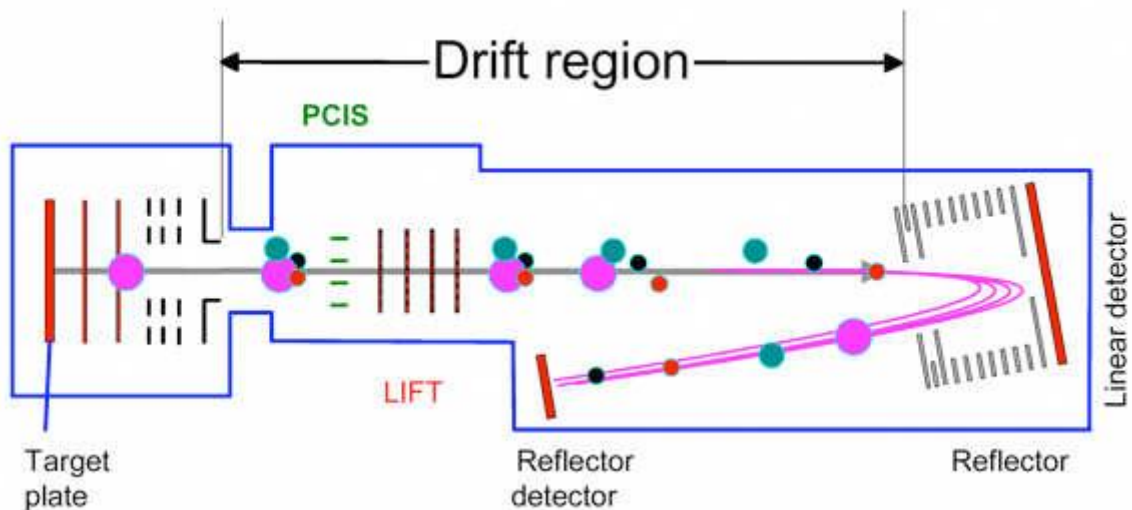


**Figure 11: Construction of an MALDI TOF/TOF MS instrument.**  
 ([http://www.giga.ulg.ac.be/jcms/cdu\\_15169/maldi-tof/tof-bruker-ultraflex-ii-tof/tof-april-2005](http://www.giga.ulg.ac.be/jcms/cdu_15169/maldi-tof/tof-bruker-ultraflex-ii-tof/tof-april-2005))

The process of peptide mass fingerprinting (PMF) means the separation of proteins typically with 1-or 2D gel electrophoresis, enzymatic in-gel digestion (using e.g. trypsin) and the analysis of samples generally with the aim of an MALDI TOF/TOF MS instrument. Protein identification by means of peptide profile is performed by correlating experimental MS spectra with theoretical spectra using database search approach, such as SEQUEST (Eng et al., 1994) or Mascot search engine (Perkins et al., 1999). The most commonly used databases are the National Center for Biotechnology Information's (NCBI) (Pruitt et al., 2005) and Swiss-Prot (Boeckmann et al., 2003). The list of matches is ranked according to the scoring scheme; the best scoring peptide match has the highest likelihood of being correct. Mascot reports a match as significant if it has a match with a less than 5% chance of being a random hit ( $p < 0.05$ ). The chance of getting a random hit is proportional to the number of sequences being searched. One way to increase significance of a hit is to reduce the number of sequences being searched by restricting the search to a specific group of species (taxonomy). The disadvantage of this sensitive and quick protein identification process is the useless in the analysis of more complex protein mixtures.

MALDI TOF/TOF MS post source decay (PSD) is fragmentation process includes laser-induced dissociation (LID) and collision-induced dissociation (CID). In case of LID no gas is added to the collision cell, only variation of the laser fluence is employed to trigger the dissociation processes (Campbell et al., 2007; Macht et al., 2004). The parent ion fragments after reacceleration in the LIFT cell but prior to it reaches the entrance of the reflectron. Analyte ions have enough energy from photoactivation and molecular collisions during the desorption process (metastable ions) but they fragment only in the mass analyzer. The precursor ion and the precursor fragments are separated by their kinetic energy. It is used for obtaining sequence information (Spengler et al., 1991).

Collision-induced dissociation (CID) is the most frequently used fragmentation method in MALDI TOF/TOF MS due to the unimolecular bond dissociations (McLuckey, 1992; Shukla and Futrell, 2000; Suckau et al., 2003). During CID, a collision is induced between the selected precursor ion and the inert argon gas molecules in the collision cell. This process is followed by the decomposition of the precursor ion. The fragments will be separated by their mass / kinetic energy (Figure 12). CID is also suitable for gaining structural, sequence informations.

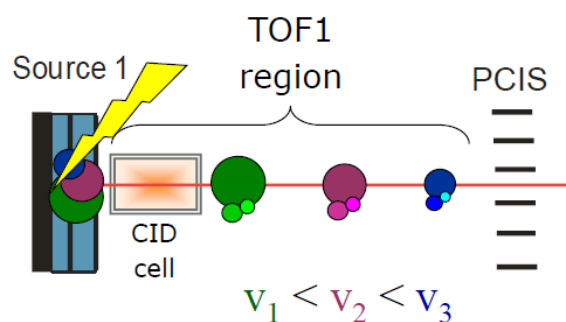


**Figure 12: CID fragmentation process. (Bruker Daltonics)**

High energy CID results mainly b-, y-ions (Figure 13), immonium ions and ions from neutral loss of ammonia and water from the b-, y-ions.

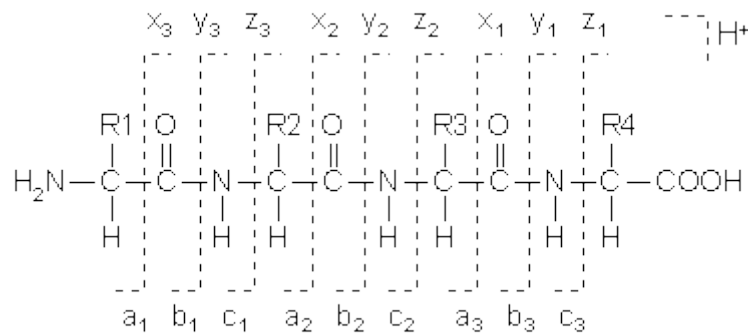


**Figure 13: Nomenclature for peptide sequencing.**

([http://www.matrixscience.com/help/fragmentation\\_help.html](http://www.matrixscience.com/help/fragmentation_help.html))

The bottom up MS/MS based protein identification method has become widely adopted (Figure 14). It is based on the digestion of proteins into peptides and the determination of their sequence using tandem mass spectrometry (MS/MS). The fragmentation pattern encoded by the MS/MS spectrum allows more precise identification of the amino acid sequence of the peptide that produced it. Sequence coverage is calculated by dividing the number of amino acids observed by the protein amino acid length. MS/MS identification is often used for protein mixtures. The MS/MS data acquisition process consists of two stages. The first stage involves reading all peptide ions that are introduced into the instrument at any given time (MS spectrum). At the second stage, selected peptide ions (often referred to as “precursor” or “parent” ions) are fragmented into smaller pieces (fragment ions). The resulting MS/MS spectra are compared with the theoretical MS/MS spectra from a protein database (NCBI, Swiss Prot) for identification.

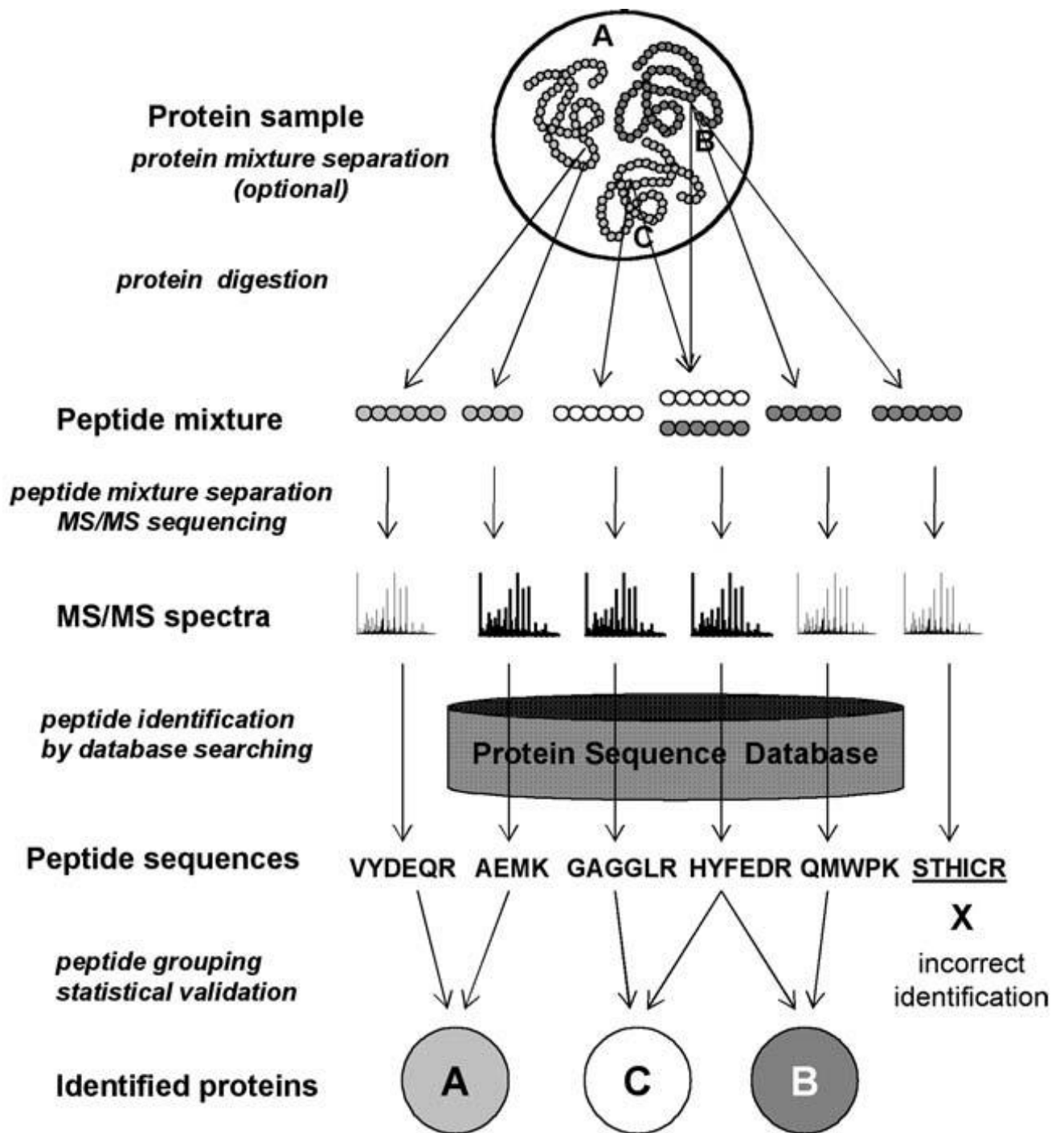


Figure 14: Steps of protein identification based on tandem mass spectrometry.  
(Matthiesen R., Mass Spectrometry Data Analysis in Proteomics)

## 4. Aims of the study

Biomarker discovery has become a crucial field of proteomics. Saliva has previously been analysed for identifying possible tumor markers by our research group. Our interest shifts towards the identification of protein-type disease biomarkers in ancient bone samples. MALDI TOF/TOF MS-based targeted peptide analysis method is cheap, non-invasive, easily automatable and high-throughput method. We investigated two different ancient diseases in archaeological human bone samples. One of them was tuberculosis, the most frequent infectious disease worldwide, caused by *Mycobacterium tuberculosis*. On the other hand osteosarcoma, a tumorous mutation was examined using mass spectrometry.

The aim of the study was:

- The extraction of ancient proteins derived from osteosarcoma and tuberculoid bone samples developing an optimized workflow.
- The separation of the extracted proteins based on their mass applying SDS gel electrophoresis.
- The mass spectrometric (MALDI TOF/TOF MS) analysis of the tryptic digested differently expressed bands (excised from the gel) compared to the control (healthy) samples.
- The identification of malignant bone tumor related molecular biomarkers and mycobacterial proteins in archaeological human skeletal remains utilizing Mascot and ProteinScape server database search engines.
- The statistical analysis of osteosarcoma, pathological (tuberculous) and non-pathological control sample cohorts.

## 5. Materials and Methods

### 5.1 Archaeological bone samples

#### 5.1.1. Osteosarcoma archaeological bone sample

The fragmented skeleton of a 25–35-year-old female with osteogenic sarcoma has been excavated at the Late Roman archaeological site of Szombathely (Savaria) - Szent Marton street 53, Hungary (municipal location code 6583/1) grave 186 (Figure 15).

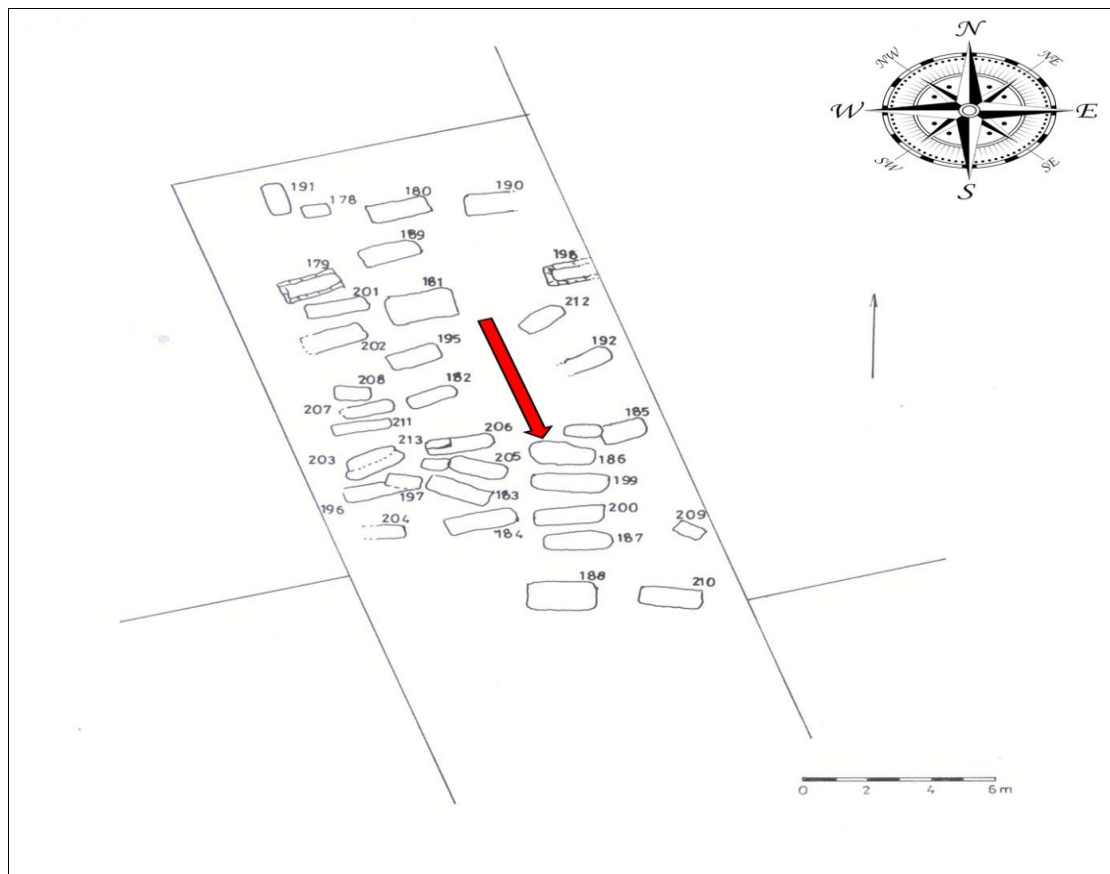


**Figure 15: The line drawing map of the archaeological site.** At this site we uncovered 33 graves from the late Roman period, arranged in four rows, very close to each other. Grave 186 (indicated with a red arrow) is located in the south-eastern section of the site, at 270-90°. The upper perimeter dimensions of the grave were 218 by 126cm, the base 185 by 120cm, with a depth of 48cm.

The analyzed bone sample was collected from the cortical region of the right humerus (Figure 16). The surface of the tumor was rough because of the irregular bone proliferation and also because of the destruction of the cortical region. The structure of the bone was typically expanded in the areas affected by the tumor.



**Figure 16: The paleoanthropological sample chosen for mass spectrometric analysis.** A) and B) Anterior and posterior views of the analyzed right humerus with osteogenic sarcoma. C) X-ray radiograph of the measured human remain. The red ellipse shows the location of the sampling.

The X-ray study demonstrates the medullary involvement, with mixed osteolytic and osteoblastic areas. Tumor infiltration of the cortex is also apparent as irregular rarefaction and lytic lesions.

The anthropological (determination of sex and age, macroscopic and morphological examinations) and paleopathological investigations (X-ray radiography) were carried out based on Knussmann (Knussmann, 1988) and Jozsa (Jozsa, 2006). A humerus from a non-cancerous skeletal remain from this cemetery (grave 199, adult female) was used for the investigations as a control sample. For further statistical validation we used our previous proteomic results of some non-pathological and *M. tuberculosis* infected bone samples (Table 1 and 2).

Location	Grave	Age	Sex	Period
Mohacs	-	Adult	Male	Recent (forensic)
Bataszek	-	Adult	Male	Recent (forensic)
Bataszek	-	Senium	Male	Recent (forensic)
Mohacs	-	Adult	Female	Recent (forensic)
Pecs	-	Adult	Female	Recent (forensic)
Hodmezovasarhely-	16	Senium	Female	Neolithic
Mezokovesd Patakrajaro	4/a	Adult	Male	Chalcolithic
Kiskundorozsma	15	Adult	Female	Bronze Age
Algyo Barakkabor	4	Mature	Male	Scythian
Szegvar Oromdulo	918	Adult	Female	Sarmatian
Kishomok	89	Mature	Female	Gepids
Szegvar Oromdulo	740	Adult	Female	Early Avar
Szekkutas Kapolnadulo	30	Adult	Female	Late Avar
Kiskundorozsma	100	Senium	Male	Hungarian Conquest
Esztergalyhorvath	284	Adult	Female	Hungarian Conquest
Kecskemet Torokfaj	65	Mature	Female	Arpad Age, X-XI <sup>th</sup> AD
Szegvar Oromdulo	617	Mature	Female	Arpad Age, XI <sup>th</sup> AD
Derekegyhaza Ibolyas	13	Senium	Male	XI-XII <sup>th</sup> AD
Csengele Bogarhat	57	Adult	Male	XIII <sup>th</sup> AD
Kecskemet Ferences	350	Adult	Female	XIV-XV <sup>th</sup> AD

**Table 1: The analyzed healthy control bone samples.**

Location	Grave	Age	Sex	Period
Sukosd-Sagod	19	Adult	Female	VII-VIII <sup>th</sup> AD
Sukosd-Sagod	19	Adult	Female	VII-VIII <sup>th</sup> AD
Bacsalmas-	39	Mature	Male	XVII <sup>th</sup> AD
Bacsalmas-	39	Mature	Male	XVII <sup>th</sup> AD
Belmegyer-Csomoki	65	Mature	Female	VIII <sup>th</sup> AD
Belmegyer-Csomoki	65	Mature	Female	VIII <sup>th</sup> AD
Csongrad-Elles	183	Mature	Male	XI-XIII <sup>th</sup> AD
Csongrad-Elles	183	Mature	Male	XI-XIII <sup>th</sup> AD
Csongrad-Elles	183	Mature	Male	XI-XIII <sup>th</sup> AD
Csongrad-Elles	183	Mature	Male	XI-XIII <sup>th</sup> AD
Csongrad-Felgyo	205	Adult	Female	VIII <sup>th</sup> AD
Csongrad-Felgyo	205	Adult	Female	VIII <sup>th</sup> AD

**Table 2: The measured pathological control (*Mycobacterium tuberculosis* infected) archaeological bone samples.**

### 5.1.2. Tuberculoid archaeological bone samples

Various *Mycobacterium tuberculosis* infected and morphologically “healthy” human skeletal remains have been analyzed from different archaeological periods. The measured paleopathological bone samples are presented in Table 3. The human bone remains were provided by the Department of Anthropology, University of Szeged, Hungary (Marcsik and Palfi, 1993; Molnar and Palfi, 1994; Palfi, 1991).

No.	Location	Grave	Age	Sex	Anatomy	Date
1	Bélmegyer-Csömöki domb	65	30-40	Female	vertebra	700-800 AD
2	Csongrád-Ellés	183	40-45	Male	vertebra	1000-1200 AD
3	Bácsalmás-Homokbánya	39	40-50	Male	vertebra	1500-1600 AD

**Table 3: Anthropological data of the measured *M. tuberculosis* infected archaeological skeletal remains.**

The paleopathological remains were investigated for DNA of *Mycobacterium tuberculosis* complex (except Csongrád-Ellés) and the test was positive in all cases (Haas et al., 2000a; Maczel, 2003; Molnar et al., 2005). Furthermore, the presence of mycolic acids as lipid biomarkers for mycobacterial infection was described previously from these archaeological bone samples as well (Mark, 2007; Mark et al., 2010). The presence of mycolic acids cannot be detected in the control samples.

## 5.2. Extraction of ancient proteins

The sample preparation, separation and mass spectrometric analysis is of a vital importance for the quality of the results. In our previous study we developed an optimized workflow for proteomic analysis of ancient proteins (Boros-Major et al., 2011) (Figure 17). The bone fragments were washed with phosphate buffer saline (PBS) and distilled water to remove contaminants. Bone powder was ground by hand using pestle and an agate mortar, the particle size was ~0.2 mm. Next, 100 mg of crude bone powder was decalcified with 1.00 ml of 0.5 M EDTA (pH=8.0), the pellet was resuspended with 100  $\mu$ l of 6 M guanidine-HCl in 0.1 M Tris (pH=7.5) at room temperature. The extraction of the proteins was carried out by continuous shaking at 4°C for 8 hours with the presence of protease inhibitor cocktail (Sigma Aldrich Kft., Budapest, Hungary).

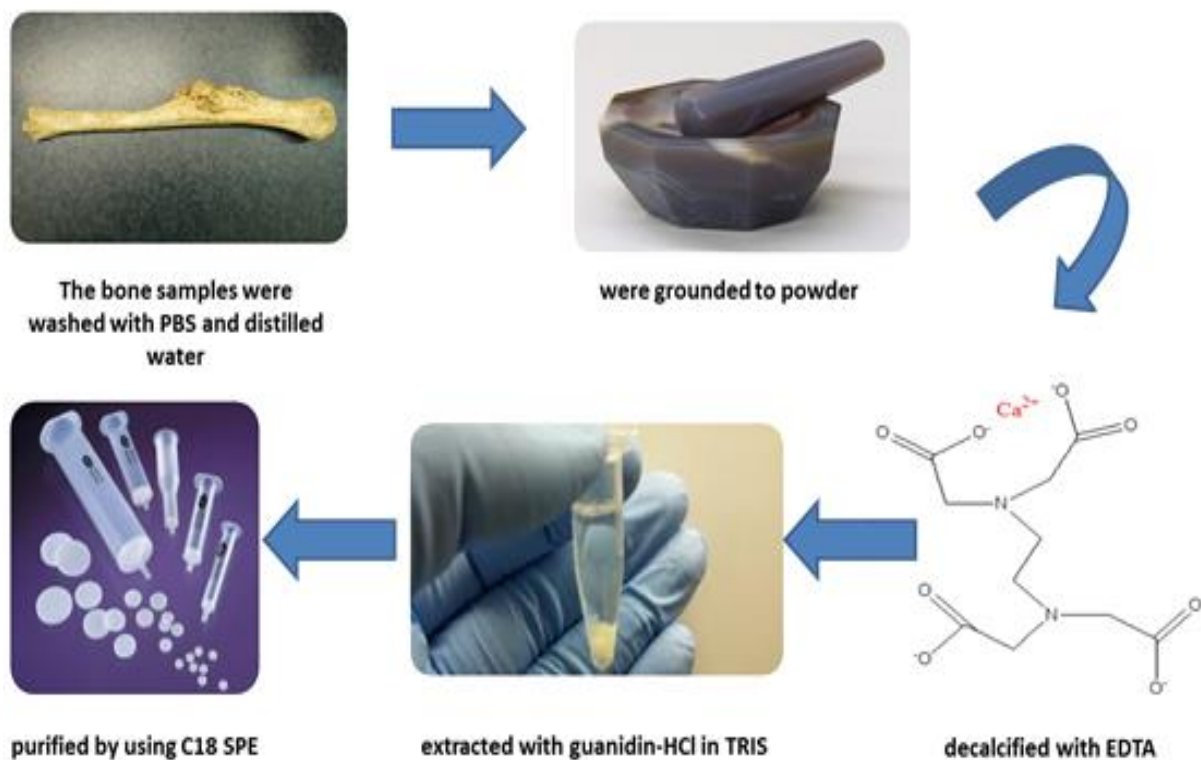


Figure 17: The steps of ancient protein extraction.

The protein extract was purified by using C18 solid phase extraction (SPE) cartridge. For this purification step a homemade octadecylsilane modified silica-based stationary phase was used with average particle size of 5  $\mu\text{m}$  and pore size of 120  $\text{\AA}$ . The stationary phase was activated with an aqueous 0.1% TFA solution, the loaded protein extract was washed with 100  $\mu\text{l}$  of 2% acetonitrile in 0.1% TFA three times. The proteins were eluted by 50  $\mu\text{l}$  of 50% acetonitrile in 0.1% TFA solution.

The solution was lyophilized to powder and stored at  $-86^{\circ}\text{C}$  until further processing. The bone sample with tumorous lesion was measured in eight technical replicates.

### 5.3. SDS-PAGE gel electrophoresis and enzymatic digestion

The lyophilized protein extract of the archaeological sample was dissolved in 100  $\mu\text{L}$  of 20 mM Tris/HCl buffer, pH 7.4 containing 3 mM EDTA, 5 mM betamercaptoethanol and 1% sodium dodecylsulphate (SDS). After the addition of 1% bromphenolblue, the samples were boiled for 2 minutes and clarified by centrifuging (8000 g for 2 min).

Sodium dodecylsulphate-polyacrylamide gel electrophoresis (SDS-PAGE) was carried out on 12% gel by Laemmli's method. A low molecular weight calibration kit (Pharmacia) was used for estimation of the molecular weight. To increase the quality of the separation and visibility of the bands the gel was run at 4°C. Gels were stained with Coomassie Brilliant Blue R-250 and destained with a solution containing 5% (v/v) acetic acid and 16% (v/v) methanol.

The bands of the overexpressed proteins (compared to the healthy archaeological samples) were excised from the gel with a razorblade, were cut into three pieces and placed in Eppendorf tubes, and destained by washing three times for 10 min in 200  $\mu\text{L}$  of 50% (v/v) acetonitrile solution containing 50 mM  $\text{NH}_4\text{HCO}_3$ . The disulphide bonds of cysteines were then reduced by 50  $\mu\text{L}$  of 20 mM dithiotreitol (DTT) in 100 mM  $\text{NH}_4\text{HCO}_3$  and acetonitrile 5% for 1 h at 55°C. The alkylation of the cysteine groups was carried out in 50  $\mu\text{L}$  of 20 mM iodoacetamide solution. The gel pieces were dehydrated at room temperature by a Speed Vac Concentrator (Speed Vac Plus, SC100A, Savant) and covered with 10  $\mu\text{L}$  of modified trypsin (Promega, Madison, WI, sequencing grade) (0.04 mg / mL) in Tris buffer (2.5 mM, pH 8.5) and left at 37°C overnight. Trypsin as a serine protease, cleaves peptide chains after lysine or arginine (except they are followed by proline).

The digestion were stopped with 15  $\mu\text{L}$  aqueous solution of acetonitrile and formic acid (49/50/1 v/v/v). The digested samples were incubated for 60 minutes at room temperature. In the last step the peptide solutions were lyophilized. The steps of in-gel digestion are shown in Figure 18.

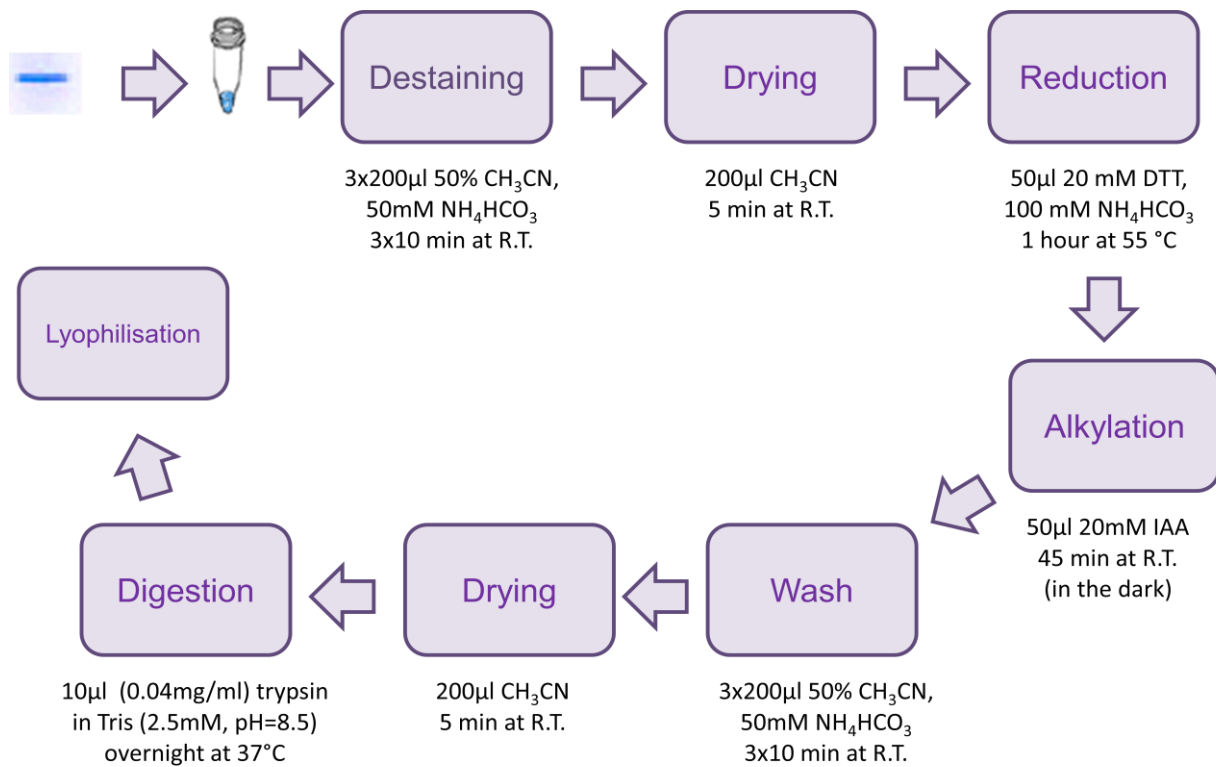


**Figure 18: Flow diagram of in-gel digestion.**

## 5.4. MALDI TOF/TOF MS-based identification of the ancient proteins

After lyophilization the samples were redissolved in 0.1% trifluoroacetic acid (TFA). The aqueous solutions of the lyophilized protein digests were concentrated and desalted by using C18 ZipTip SPE pipette tips (Millipore Kft, Budapest, Hungary). Then the purified peptides were eluted directly onto the target plate (MTP 384 massive target T, Bruker Daltonics, Bremen, Germany) by using of 3  $\mu$ L of a saturated matrix solution, prepared fresh every day by dissolving  $\alpha$ -cyano-4-hydroxycinnamic acid (CHCA) in acetonitrile/ 0.1% TFA (1/2, v/v). The mass spectrometer used in this work was an Autoflex II TOF/TOF (Bruker Daltonics, Bremen, Germany) operated in reflectron mode for peptide mass fingerprinting (PMF) or in LIFT mode for LID (laser induced decay) and CID (collision induced decay) fragmentation. The accelerating voltage was set to 20.00 kV. The instrument uses a 337 nm nitrogen laser (model MNL-205MC, Lasertechnik Berlin GmbH., Berlin, Germany). External calibration was performed in each case using Bruker Peptide Calibration Standard (#206195 Peptide Calibration Standard, Bruker Daltonics, Bremen, Germany). Peptide masses were acquired in the range of m/z 700 to m/z 5000. Each spectrum was produced by accumulating data from at least 500 consecutive laser shots. The FlexControl 2.4 software (Bruker Daltonics, Bremen, Germany) was used to control the instrument and FlexAnalysis 2.4 software (Bruker Daltonics, Bremen, Germany) was used for spectra evaluation. Singly charged monoisotopic peptide masses were searched against Swiss-Prot and NCBI nr databases (last accessed: 11/19/2012) by utilizing the MASCOT database search engine (version 2.2) ([www.matrixscience.com](http://www.matrixscience.com), Matrix Science Ltd., London, UK), Bruker BioTools 3.0 software (Bruker Daltonics, Bremen, Germany) and Bruker ProteinScape server 2.1 (Bruker Daltonics, Bremen, Germany). Maximum one missed tryptic cleavage was considered, and the mass tolerance for monoisotopic peptide masses was set to 80 ppm carbamidomethylation was set as global modification while methionine oxidation was set as variable modification. Additionally LID and CID fragmentation of the matched peptides were carried out for MALDI TOF/TOF MS to provide further evidence for the presence of the identified proteins.

## 5.5. Statistical analysis

Mass spectrometric techniques play an emerging role in biomarker research due to their high mass accuracy, sensitivity, and speed of detection. The ClinProTools software builds on mass spectrometric results and allows researchers to directly evaluate peptide/protein profiles derived from different clinical samples. The ClinProTools software provides highly sophisticated bioinformatics tools, multivariate statistics enables the analysis and discovery of hidden and complex peak patterns leading to class prediction.

Statistical analysis was carried out only to demonstrate the predictive value of the identified biomarkers the mass spectrometric results were statistically evaluated by ClinProTools 2.2 (Bruker Daltonics, Bremen, Germany) clustering software. Multiple spectra of the analyzed bone samples from different sample cohorts, such as osteosarcoma, non-pathological and pathological (tuberculous) control samples were distinguished together. Recalibration, spectral alignment, peak normalization, peak detection and peak area calculation of spectra were carried out automatically by ClinProTools. A logistic regression model was performed to identify the significant predictive peaks on the basis of the normalized peak areas. Wilcoxon signed-rank test was used for non-parametric statistical analysis of the different sample cohorts.

The Wilcoxon rank-sum test is a non-parametric alternative to the paired Student's t-test. The null hypothesis tested is that a sample is symmetrically distributed around a specified center. Scores exactly equal to the central point are excluded and the absolute values of the deviations from the central point of the remaining scores are ranked such that the smallest deviation has a rank of 1. Tied scores are assigned for a mean rank. The sums for the ranks of scores with positive and negative deviations from the central point are then calculated separately. A value  $S$  is defined as the smaller of these two rank sums.  $S$  is then compared to a table of all possible distributions of ranks to calculate  $p$ , the statistical probability of attaining  $S$  from a population of scores that is symmetrically distributed around the central point. As the number of used scores,  $n$ , increases, the distribution of all possible ranks  $S$  tends towards the  $z$ -distribution, so for an  $n$  of greater than 10 this distribution is used to calculate  $p$ . This test assumes that the compared sample sets originate at least from a common distribution.

## 6. Results and Discussion

### 6.1. Osteogenic Sarcoma

This work partly focused on the identification of possible protein biomarkers of osteogenic sarcoma from a 2000-year-old anthropological sample. The proteins were separated by 1D gel electrophoresis (Figure 19) and the interested bands were enzymatically digested.

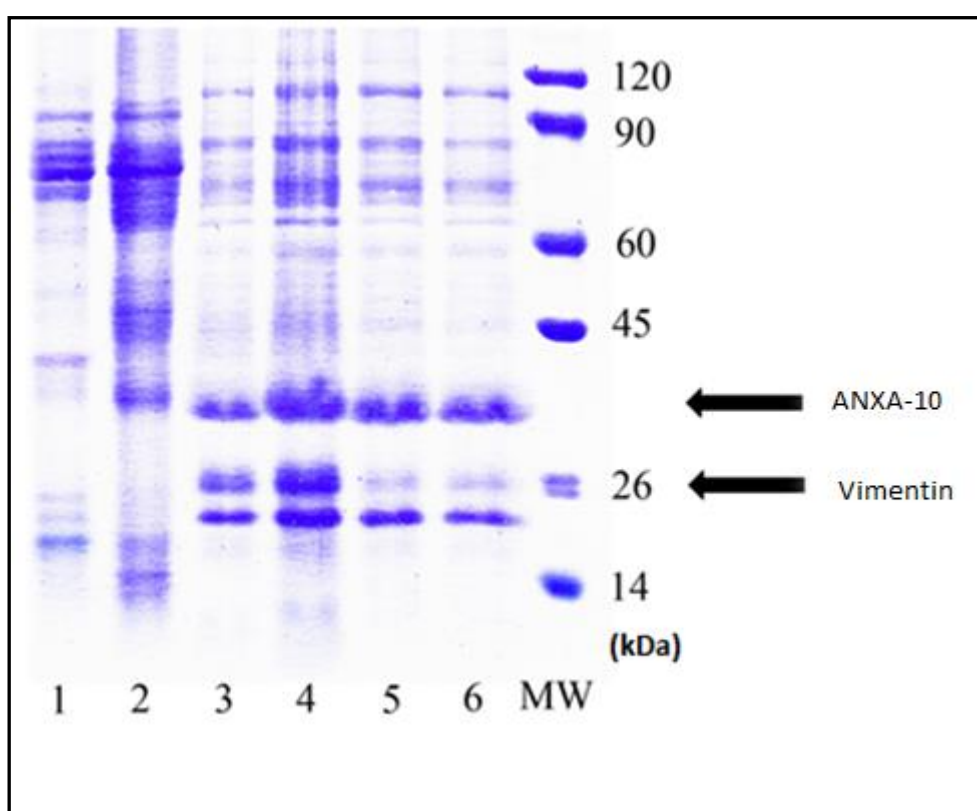


**Figure 19: Characteristic 1D SDS PAGE electrophoretogram of healthy control and the pathological bone samples.** Lanes 1 and 2 are healthy control samples from Hodmezovasarhely-Gorzsa and Szegvar-Oromdulo, lanes 3–6 are osteosarcoma samples. Arrows show the bands of Annexin A10 (37.3 kDa) and Vimentin (26.8 kDa). The parameters of the separation are mentioned in the text.

The tryptic peptides were analyzed by MALDI TOF/TOF MS and the identification of the resulted proteins was carried out using a PMF or MS/MS search. Based on our results several known, previously published osteosarcoma or tumor related proteins and gene products were detected from the ancient pathological bone sample (Table 4).

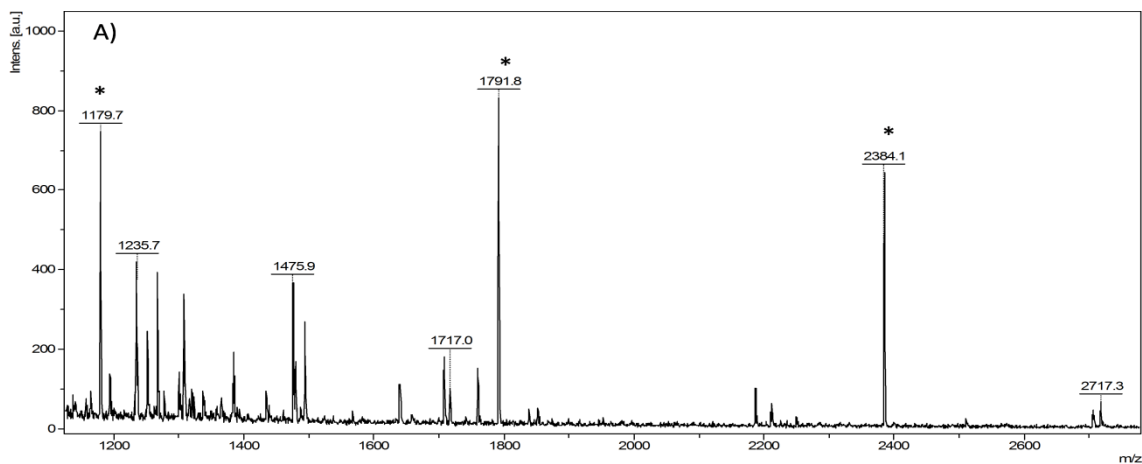
Accession	Name	MW [kDa]	Peptides	SC [%]
AK1A1_HUMAN	Alcohol dehydrogenase (NADP+)	36,5	5	14,2
gi 225939	aldehyde reductase	36,3	5	14,2
gi 48762937	annexin A10	37,3	8	27,2
gi 62087532	arginine/serine-rich splicing factor 6 variant	31,8	6	27,6
ARI5B_HUMAN	AT-rich interactive domain-containing protein 5B	132,2	11	13,0
gi 33878074	BAT2 protein	17,1	5	29,9
gi 49456879	BCL2A1	20,3	7	44,0
VMDL3_HUMAN	Bestrophin-4	76,1	7	14,5
gi 882391	bone morphogenic protein type II receptor	59,9	6	13,2
S10AB_HUMAN	Calgizzarin (S100 calcium-binding protein A11)	11,7	4	43,8
CAN7_HUMAN	Calpain-7	92,6	7	12,3
K1C10_HUMAN	Cytokeratin 10	59,5	14	23,1
gi 33188433	deleted in liver cancer 1 isoform 1	170,5	13	7,9
gi 28704113	DHX8 protein	138,7	13	13,8
G59435	DLC-1	122,7	10	10,9
DNL3_HUMAN	DNA ligase III	102,6	10	16,3
TDT_HUMAN	DNA nucleotidylexotransferase	58,4	9	22,2
MP2K6_HUMAN	Dual specificity mitogen-activated protein kinase kinase 6	37,5	7	23,4
DTNA_HUMAN	Dystrobrevin alpha	83,9	6	10,5
gi 15010856	galectin-12 isoform d	30,0	5	30,5
GCC2_HUMAN	GRIP and coiled-coil domain-containing protein 2	184,5	18	12,3
gi 40555827	heat shock factor protein 2 isoform c	27,0	7	23,9
HSPB6_HUMAN	Heat-shock protein beta-6	17,1	5	35,0
CAC10772	Immunoglobulin heavy chain variable region	12,4	5	65,5
gi 17318569	keratin 1	66,0	15	25,8
Q8N175_HUMAN	Keratin 10	58,8	14	23,5
gi 31559819	keratin 25C	49,8	8	17,2
gi 47132620	keratin 2a	65,4	9	16,4
CAA82315	keratin 9	62,1	11	16,9
A44861	keratin, 67K type II epidermal	65,8	9	16,3
K1C9_HUMAN	Keratin, type I cytoskeletal 9	61,9	11	20,7
AAP97338	Methyl-CpG-binding domain protein 4	60,9	13	16,3
NEBL_HUMAN	Nebulette	116,4	14	16,7
NRAP_HUMAN	Nebulin-related-anchoring protein	197,0	24	14,9
gi 4506335	parvalbumin	12,1	8	56,4
PRVA_HUMAN	Parvalbumin alpha	11,9	8	56,9
gi 39653323	PHD finger protein 20-like 1 isoform 1	47,7	7	15,8
gi 39653321	PHD finger protein 20-like 1 isoform 3	16,6	6	42,0
gi 31873386	phospholipase C	39,7	7	30,7
gi 346323	phosphoprotein phosphatase (EC 3.1.3.16) X catalytic chain	35,1	6	26,1
PDIP2_HUMAN	Polymerase delta-interacting protein 2	42,0	7	22,0
CAF00150	Proteasome subunit beta type 3	16,6	5	34,9
gi 565647	proteasome subunit Hsc10-II	22,9	5	25,4
PARK7_HUMAN	Protein DJ-1 (Oncogene DJ1)	19,9	5	32,3
gi 55859594	PTAR1 protein	32,4	7	30,1
gi 4960030	Rab GDP dissociation inhibitor beta	41,0	6	22,0
gi 39841018	RAB GTPase activating protein 1-like	92,5	8	10,3
gi 537327	receptor tyrosine kinase	18,5	6	30,0
gi 2665850	rheumatoid factor RF-ET7	10,9	6	74,5
RHG07_HUMAN	Rho GTPase-activating protein 7	122,7	10	10,9
gi 41152086	serine (or cysteine) proteinase inhibitor, clade B (ovalbumin), member 6	42,6	9	29,3
gi 38382764	SET-binding protein isoform b	26,4	7	25,6
gi 46250431	Transcription factor NRF	77,7	11	20,4
gi 62088924	Transducin-like enhancer of split 3 splice variant 1 variant	22,9	6	37,1
gi 37747855	Transferrin	77,0	10	21,9
gi 4507659	translocated promoter region (to activated MET oncogene)	265,4	24	12,0
gi 4827050	ubiquitin specific protease 14	56,0	8	20,6
gi 71774197	ubiquitin specific protease 47	147,1	10	13,4
gi 34532272	unnamed protein product (homolog of CCDC144A protein)	56,3	12	21,9
gi 21754902	unnamed protein product (homolog of Zinc finger protein 781)	17,8	7	48,7
gi 57471648	vimentin	26,8	8	38,2
WBP4_HUMAN	WW domain-binding protein 4	42,5	7	15,7
ZN224_HUMAN	Zinc finger protein 224	82,2	10	19,4
gi 74355161	Zinc finger protein 624	85,6	11	22,5

**Table 4: The identified up-regulated proteins from 2000-year-old osteogenic sarcoma. (Mascot score > 50)**

The identified annexins (ANXs) are calcium and phospholipid binding proteins, they play a crucial role in the exocytic and endocytic transport, regulation of cell growth, proliferation and apoptosis. It is well known, that the increased level of ANXs (ANXA-10) indicates tumor progression (Kim et al., 2010; Shimizu et al., 2012). The B-cell lymphoma 2-related protein A1 (BCL2A1) is a member of BCL2 proteins. BCL2A1 is responsible for the separation of pro-apoptotic BCL2 proteins. BCL2A1 shows an elevated level in case of different cancer types such as leukemia and lymphoma, also connected with autoimmunity and therapy resistance of different tumors (Bolden et al., 2013; Ottina et al., 2012; Vogler, 2012; Willimott and Wagner, 2012). Calgizzarin (S100A11) belongs to the calcium binding proteins S100 family, involved in cell growth, motility and differentiation. Calgizzarin has been correlated with tumor progression and metastasis (Melle et al., 2006; Rehman et al., 2004). DLC1 is a known tumor suppressor, acting through Rho GTPase-activating protein (RhoGAP), which is involved in the proliferation and migration of tumor cells, induces apoptosis in vitro (Kim et al., 2009; Yang et al., 2011; Zhang et al., 2009). Heat-shock protein's (HSP's) expression increases in case of thermal, physiological or other stress factors allowing the cells to survive lethal conditions. HSP's play key role in the apoptotic and cell death process (inhibition of caspase activation). Elevated level of HSP beta-6 was found in clinical samples of patients who suffered from osteosarcoma (Folio et al., 2009; Suehara et al., 2012). DJ-1 protein is a mitogen-dependent oncogene involved in ras-related signal transduction pathway. Overexpression of DJ-1 indicates tumorous mutation (Niforou et al., 2008; Tian et al., 2008). The RhoGAP family proteins play an important role in regulating cell migration, cell morphology and cytoskeletal organization. Down regulation of RhoGAP proteins decrease the tumor suppressive effect (Li et al., 2009). Transferrin is a member of iron-binding blood plasma glycoproteins, which is responsible for the regulation of the free iron content in the blood. Elevated level of transferrin is correlated with tumorous diseases such as osteosarcoma (Li et al., 2010; Suehara et al., 2012). The expression of a cytoskeletal intermediate filament protein vimentin (VIM) was also shown to increase in case of osteosarcoma (Flores et al., 2012; Kang et al., 2006; Li et al., 2010; Suehara et al., 2012) VIM is considered to be a tumor biomarker, as it is promoting the metastatic spread of the tumor cells. In this study, some keratins were identified as well. The origin and the importance of these proteins are not well known; probably the identified keratins are from recent or contemporary

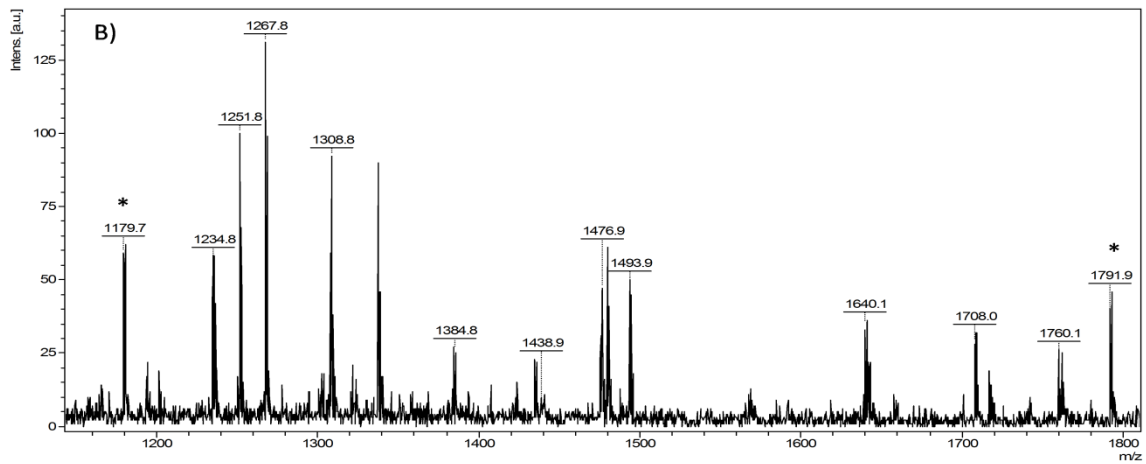
contaminations. However, the up-regulation of cytokeratins has been published in U2OS osteosarcoma specific cell line (Niforou et al., 2008).

Representative mass spectra and the list of the identified tryptic peptides of annexin A10 and vimentin are showed on Figure 20. The results show characteristic peaks of the identified biomarkers, however some keratin peaks are present on the spectra. This pollution is common from ancient bone tissue, but various types of keratins are up-regulated in different tumors as well.



Position	Molecular mass (Da)	Sequence	MS/MS	Modification
81-103	2717.24	DVMAGLMYPPPLYDAHELWHAMK		
193-202	1194.69	TMLQMILCNK	+	
193-202	1251.68	TMLQMILCNK		CAM(C)
193-202	1267.72	TMLQMILCNK		CAM(C)+ OX(M)
212-227	1760.66	QEFQNISGQDMVDAIN		
233-243	1234.78	VDAINECYDGY		
293-302	1235.60	YGKSLFHDR	+	
296-310	1791.73	SLFHDIRNFASGHYK		
311-324	1716.95	KALLAICAGDAEDY	+	
313-324	1475.87	LLAICAGDAEDY	+	

**Figure 20: Representative mass spectra and the list of the identified tryptic peptides of two identified tumor biomarkers. A) Annexin A10, B) Vimentin. Some keratin contamination has been detected in the sample, the tryptic peptides of keratin were used as internal calibration standards and the peaks are marked with asterisk.**



Position	Molecular mass (Da)	Sequence	MS/MS	Modification
3-14	1639.91	NCFRLQEMLQR	+	CAM(C)+ OX(M)
15-25	1323.66	EEAENTLQSFR		
89-100	1393.71	DVRQQYESVAAK		
111-122	1308.64	SKFADLSEAANR	+	
209-220	1439.79	MALDIEIATYRK		OX (M)
220-228	1060.63	KLLEGEESR		

Figure 20 (continued)

Based on our statistical analysis the different sample cohorts such as osteosarcoma, healthy control and tuberculous control could be distinguished, using two peptide peaks ( $m/z$  1180, 1385) derived from the investigated osteogenic bone sample. The spectral profile of the samples with osteosarcoma is significantly different as the other two group's profiles (Figure 21).

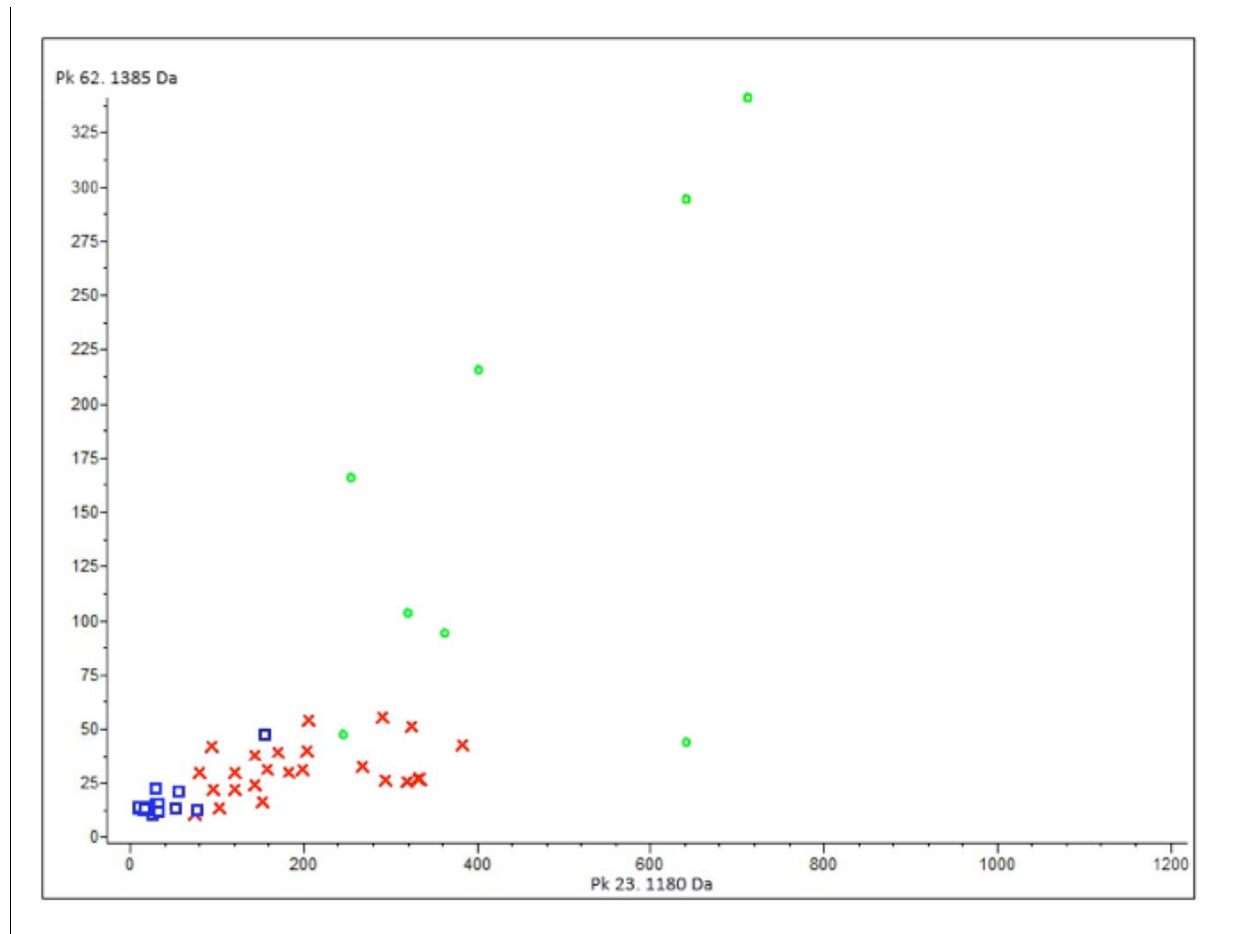


**Figure 21: ClinProTools-based Wilcoxon non-parametric statistical test of different sample cohorts.** Cluster analysis from sample sets of the osteosarcoma (green), healthy control sample (red) and tuberculous control sample (blue) groups using the peptide peaks with  $m/z$  1180 and 1385. The x-and y-axes correspond to the relative intensities of the peptide peaks.

## 6.2. Tuberculosis

Further target of our interest was the identification of ancient mycobacterial proteins. The protein bands were excised and digested with trypsin, and the resulting peptides were analyzed by MALDI TOF/TOF MS for protein determination. The identifications of *Mycobacterium* specific proteins using peptide mass fingerprint (PMF) analysis and direct sequencing of the tryptic peptides were successful in all investigated tuberculosis infected archaeological bone samples.

The proteomic results from the oldest investigated bone sample (Bélmegyer-Csömöki domb) have been showed in Table 5.

Protein ID	Accession no.	Theoretical MW (Da)	Mascot score	Peptides matched	Sequence coverage (%)
Adenylate kinase ( <i>M. tuberculosis</i> )	gi 15607873	20113	263	14	65
Hypothetical protein ( <i>M. tuberculosis</i> )	gi 254232569	50448	71	8	15
LysR family transcriptional regulator ( <i>M. tuberculosis</i> )	gi 15607518	33616	68	8	29
Putative helicase ( <i>M. tuberculosis</i> )	gi 260187090	111734	113	19	25
Translation initiation factor IF-2 ( <i>M. tuberculosis</i> )	gi 215431780	54012	95	10	32

**Table 5: Proteomic parameters of the identified mycobacterial proteins of the archaeological skeletal remain from Bélmegyer-Csömöki domb grave 65.** Experimental conditions were mentioned in the text.

In this sample numerous mycobacterial proteins were identified such as adenylate kinase, LysR family transcriptional regulator protein, putative helicase, translation initiation factor IF-2 protein and a hypothetical protein. A characteristic mass spectrum has been displayed in Figure 22.

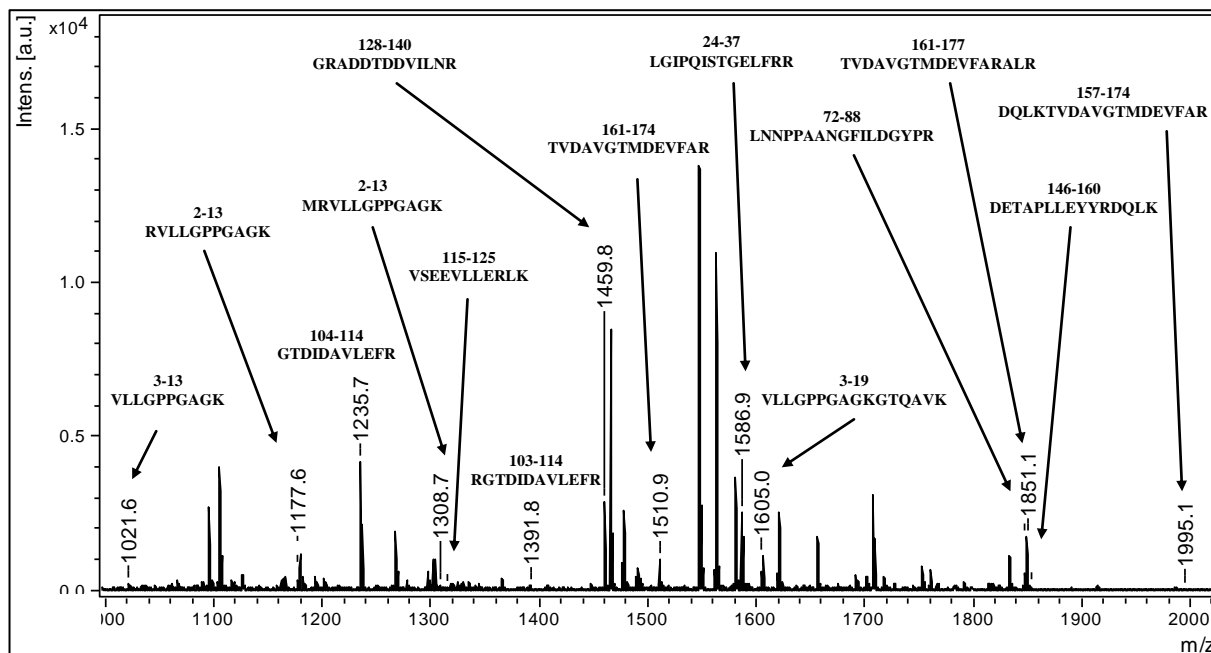


**Figure 22: Mass spectra of skeletal remain from Bélmegyer-Csömöki domb grave 65.**

The *Mycobacterium tuberculosis* related proteomic results of the other two archaeological sites (Csongrád-Ellés and Bácsalmás-Homokbánya) have been summarized in Table 6 and 7.

In these cases several microbial enzymes (catalase-peroxidase-peroxinitritase-T katG, dehydrogenase/reductase, fumarate reductase flavoprotein subunit, glycosyl transferase, oxidoreductase, peptide sythetase nrp) as well as mycobacterial regulatory and hypothetical proteins were identified.

Protein ID	Accession no.	Theoretical MW (Da)	Mascot score	Peptides matched	Sequence coverage (%)
Catalase-peroxidase-peroxinitritase-T katG ( <i>M. tuberculosis</i> )	gi 219557862	51220	62	8	24
Fumarate reductase flavoprotein subunit ( <i>M. tuberculosis</i> )	gi 15608690	63723	163	18	34
Hypothetical protein ( <i>M. tuberculosis</i> )	gi 15843166	37267	85	10	28
Oxidoreductase ( <i>M. tuberculosis</i> )	gi 15610689	36808	86	10	28
Peptide synthetase nrp ( <i>M. tuberculosis</i> )	gi 254233496	269241	122	23	11

**Table 6: Proteomic parameters of the identified mycobacterial proteins of the archaeological skeletal remain from Csongrád-Ellés grave 183. Experimental conditions were mentioned in the text.**

Protein ID	Accession no.	Theoretical MW (Da)	Mascot score	Peptides matched	Sequence coverage (%)
Dehydrogenase/reductase ( <i>M. tuberculosis</i> )	gi 218751933	32749	101	10	40
Fumarate reductase flavoprotein subunit ( <i>M. tuberculosis</i> )	gi 15608690	63723	113	15	30
Glycosyl transferase ( <i>M. tuberculosis</i> )	gi 218754716	20715	91	9	47
Hypothetical protein ( <i>M. tuberculosis</i> )	gi 215428650	36324	93	12	31
Regulatory protein ( <i>M. sp. JLS</i> )	gi 126436787	28284	119	8	43

**Table 7: Proteomic parameters of the identified mycobacterial proteins of the archaeological skeletal remain from Bácsalmás-Homokbánya grave 39. Experimental conditions were mentioned in the text.**

Tuberculoid bone samples represent different eras and different regions of Hungary and that serves as an explanation for the difference between the protein profiles.

In the case of the morphologically “healthy” control samples various types of human keratins, collagens were detected, but *M. tuberculosis* proteins cannot be identified.

The suggested proteomic approach by using tandem mass spectrometric sequencing of the peptides can be feasible for species identification as previously described in zoological samples (Buckley et. al., 2008a, 2009). All identified bacterial proteins are from human pathogen *Mycobacterium* species and consequently, the contamination with other e.g. soil living mycobacteria can be easily controlled and eliminated by using their different amino acid sequences. Namely, the taxa specific distinguishing of the referred and partly sequenced mycobacterial proteins can be easily carried out by using their exact amino acid sequences and the homology search of the proteins and peptides (e.g. NCBI BLAST).

## 7. Conclusions

- Osteosarcoma and tuberculosis-related proteins were identified from archeological bone samples using MALDI TOF/TOF MS for the first time.
- One of our goals was to find potential tumor biomarkers for ancient osteosarcoma using healthy bone samples as a control. Using an appropriate extraction method, developed by our research group, followed by SDS PAGE, tryptic digestion and MALDI TOF/TOF MS analysis, we were able to identify several proteins that were tightly connected to tumorous mutations. The overexpression of annexin A10 protein, BCL-2-like protein, calgizzarin, HSP beta-6, RhoGAP-activating protein 7, transferrin, and vimentin among others referred to healthy samples may indicate the presence of tumor in bones.
- In this study, we demonstrated that the peptide profile of the samples with osteosarcoma is statistically unique and it could be distinguished from other sample cohorts such as non-pathological (healthy) and pathological (tuberculous).
- On the basis of our results the proteomic analyses could indicate the presence of osteosarcoma in bone tissues. Our findings showed that the well known, osteosarcoma-related clinical protein biomarkers are detectable in the investigated 2000-year-old tumorous skeletal remain. In the future, additional comparative proteomic investigations are needed for the further early stage biomarker discovery of ancient primary bone cancer.
- As further target of our investigations several mycobacterial proteins have been extracted and identified by MALDI TOF/TOF MS from archaeological human skeletal remains also for the first time.

- Our results suggest that the protein extraction, purification and identification from ancient skeletal remains can be carried out not only for the most abundant bone proteins, but also at the subproteome level. The identification of *Mycobacterium tuberculosis* proteins as molecular biomarkers avoids the recent problems of PCR-based mycobacterial aDNA analysis. The presented MS-based proteomic method provides species specific results, accordingly the different human pathogens (e.g. *M. tuberculosis*, *M. bovis*, *M. leprae*) can be distinguish together with this technique, furthermore the negative effect of the possible recent and contemporary contaminations can be minimized.

The present studies showed, that the MS-based protein analysis of the ancient proteins is a powerful technique for paleopathological examinations. It is a well known fact that the evolution of *M. tuberculosis* as well as *M. leprae* is unclarified. This complex problem can be feasible by using proteomics and genomics of the recent and ancient strains. Moreover, the paleoproteomic analysis can be an independent, robust, high-throughput technique for confirmation of the presents of human pathogen *Mycobacterium* species.

Our proteomic results could enhance the diagnosis of osteogenic tumors in ancient human skeletal remains. Furthermore the identification and sequencing of ancient mycobacterial proteins with further biomolecular techniques (aDNA, determination of lipid biomarkers) have the potential to expand our understanding of ancient epidemiology and evolution of these pathogens.

## 8. Acknowledgements

This work was supported by GVOP 0179, DDEK Kft., SciEx Kft., Hungarian National Scientific Research Foundation (OTKA Grant No. K72592, CNK78480, D048294, CK80179, NN109841, K104984), European Union and State of Hungary (TIOP 1.3.1-10/1-2010-0008, TIOP 1.3.1-07/1, SROP-4.2.2.A-11/1/KONV-2012-0053) and PTE AOK KA 34039-2009, 2011, 2012-2013 (13-18).

I would like to thank Dr. László Márk, my theme leader and Prof. Balázs Sümegi, my PhD program leader for supporting my work with excellent ideas and financially as well.

I am grateful to Prof. Dóra Reglődi and Prof. Ákos Vértes for their helpful comments and for the revision of my article.

I thank my colleagues Éva Jámber, Dr. Katalin Fekete, János Schmidt, Dr. Gábor Maász, Dr. Zoltán Pápai, Dr. Péter Avar, Dóra Petrovics and Dr. Katalin Böddi for their help and friendly support.

I am thankful to Erika Szemmelróthné and Anita Horváth for the technical help I received.

I would also like to thank everyone who is not listed above but contributed to my research.

## 9. References

Arriaza BT, Salo W, Aufderheide AC, Holcomb TA. Pre-Columbian tuberculosis in northern Chile: molecular and skeletal evidence. *Am J Phys Anthropol.* 1995;98(1):37-45.

Asara JM, Schweitzer MH, Freimark LM, Phillips M, Cantley LC. Protein sequences from mastodon and *Tyrannosaurus rex* revealed by mass spectrometry. *Science.* 2007;316:280-5.

Asara JM, Garavelli JS, Slatter DA, Schweitzer MH, Freimark LM, Phillips M, et al. Interpreting sequences from mastodon and *T. rex*. *Science.* 2007;317(5843):1324-5.

Atkins D, Lichtenfels R, Seliger B. Heat shock proteins in renal cell carcinomas. *Contrib Nephrol.* 2005;148:35-56.

Aufderheide AC, Ragsdale B, Buikstra J, Ekberg F, Vinh TN Structure of the radiological “sunburst” pattern as revealed in an ancient osteosarcoma. *Journal of Paleopathology.* 1997;9:101–6.

Beckingsale TB, Gerrand GH. Osteosarcoma. *Orthopaedics and Trauma.* 2010;24:321–31.

Beverly LJ, Varmus HE. MYC-induced myeloid leukemogenesis is accelerated by all six members of the antiapoptotic BCL family. *Oncogene.* 2009;28(9):1274-9.

Blondiaux J. Etude des ossements humains de la crypte de l’Eglise 12 CAPASSO Saint-Gery ou Mont des Boeufs a Cambrai. *Revue du Nord* 1986;68:385–392. (in French).

Bocca C, Ievolella M, Autelli R, Motta M, Mosso L, Torchio B, et al. Expression of Cox-2 in human breast cancer cells as a critical determinant of epithelial-to-mesenchymal transition and invasiveness. *Expert Opin Ther Targets.* 2014;18(2):121-35.

Boeckmann B, Bairoch A, Apweiler R, Blatter MC, Estreicher A, Gasteiger E, et al. The SWISS-PROT protein knowledgebase and its supplement TrEMBL in 2003. *Nucleic Acids Res.* 2003;31(1):365-70.

Bolden JE, Shi W, Jankowski K, Kan CY, Cluse L, Martin BP, et al. HDAC inhibitors induce tumor-cell-selective pro-apoptotic transcriptional responses. *Cell Death Dis.* 2013;4:e519.

Boros-Major A, Bona A, Lovasz G, Molnar E, Marcsik A, et al. New perspectives in biomolecular paleopathology of ancient tuberculosis: a proteomic approach. *J. Archaeol. Sci.* 2011;38:197–201.

Brothwell D. The evidence of neoplasms. In: Brothwell D, Sandison T, eds. *Diseases in antiquity*. Springfield: CC Thomas 1967:320–45.

Brothwell D. *Digging up bones*. London: Oxford University Press 1981:139–43.

Buckley M, Collins M, Thomas-Oates J. A method of isolating the collagen (I) alpha2 chain carboxytelopeptide for species identification in bone fragments. *Anal Biochem.* 2008a;374(2):325-34.

Buckley M., Anderung C., Penkman K., Raney B.J., Götherström A., Thomas-Oates J., Collins M. Comparing the survival of osteocalcin and mtDNA in archaeological bone from four European sites. *J. Archaeol. Sci.* 2008b;35:1756-64.

Buckley M, Collins M, Thomas-Oates J, Wilson JC. Species identification by analysis of bone collagen using matrix-assisted laser desorption/ionisation time-of-flight mass spectrometry. *Rapid Commun Mass Spectrom.* 2009;23(23):3843-54.

Buckley M, Kansa SW, Howard S, Campbell S, Thomas-Oates J, Collins M. Distinguishing between archaeological sheep and goat bones using a single collagen peptide. *J. Archaeol. Sci.* 2010;37:13-20.

Campbell JM, Vestal ML, Blank PS, Stein SE, Epstein JA, Yergey AL. Fragmentation of leucine enkephalin as a function of laser fluence in a MALDI TOF-TOF. *J Am Soc Mass Spectrom.* 2007;18(4):607-16.

Campillo D. *Lesiones patológicas en craneos prehistoricos de la region valenciana*. Valencia: S.I.P. So. 93, 1976. (in Spanish)

Capasso L, Di Muzio M, Di Tota G, Spoletini L. A case of probable cranial Hemangioma (Iron Age, Central Italy). *Journal of Paleopathology*. 1992;4: 55–62.

Cappellini E, Jensen LJ, Szklarczyk D, Ginolhac A, da Fonseca RA, Stafford TW, et al. Proteomic analysis of a pleistocene mammoth femur reveals more than one hundred ancient bone proteins. *J Proteome Res*. 2012;11(2):917-26.

Chen JH, Ni RZ, Xiao MB, Guo JG, Zhou JW. Comparative proteomic analysis of differentially expressed proteins in human pancreatic cancer tissue. *Hepatobiliary Pancreat Dis Int*. 2009;8(2):193-200.

Chen XJ, Carroll JA, Beavis RC. Near-UV-induced matrix-assisted laser desorption/ionization as a function of wavelength. *J. Am. Soc. Mass Spectrom*. 1998;9 (9):885–91.

Choi SS, Park IC, Yun JW, Sung YC, Hong SI, Shin HS. A novel Bcl-2 related gene, Bfl-1, is overexpressed in stomach cancer and preferentially expressed in bone marrow. *Oncogene*. 1995;11(9):1693-8.

Ciocca DR, Calderwood SK. Heat shock proteins in cancer: diagnostic, prognostic, predictive, and treatment implications. *Cell Stress Chaperones*. 2005;10(2):86-103.

Cross SS, Hamdy FC, Deloulme JC, Rehman I. Expression of S100 proteins in normal human tissues and common cancers using tissue microarrays: S100A6, S100A8, S100A9 and S100A11 are all overexpressed in common cancers. *Histopathology*. 2005;46(3):256-69.

Crubézy E, Legal L, Fabas G, Dabernat H, Ludes B. Pathogeny of archaic mycobacteria at the emergence of urban life in Egypt (3400 BC). *Infect Genet Evol*. 2006;6(1):13-21.

Crubézy E, Ludes B, Poveda JD, Clayton J, Crouau-Roy B, Montagnon D. Identification of Mycobacterium DNA in an Egyptian Pott's disease of 5,400 years old. *C R Acad Sci III*. 1998;321(11):941-51.

Dastugue J Tumeur maxillaire sur un crane du Moyen-Age. *Bulletin de l'Association francaise pour l'etud du cancer*. 1965;52: 69–72. (in French)

Deng S, Jing B, Xing T, Hou L, Yang Z. Overexpression of annexin A2 is associated with abnormal ubiquitination in breast cancer. *Genomics Proteomics Bioinformatics*. 2012;10(3):153-7.

Deng Z, Du WW, Fang L, Shan SW, Qian J, Lin J, et al. The intermediate filament vimentin mediates microRNA miR-378 function in cellular self-renewal by regulating the expression of the Sox2 transcription factor. *J Biol Chem*. 2013;288(1):319-31.

Donoghue HD, Marcsik A, Matheson C, Vernon K, Nuorala E, Molto JE, et al. Co-infection of *Mycobacterium tuberculosis* and *Mycobacterium leprae* in human archaeological samples: a possible explanation for the historical decline of leprosy. *Proc Biol Sci*. 2005;272(1561):389-94.

Donoghue HD, Herskovitz I, Minnikin DE, Besra GS, Lee OY, Galili E, et al. Biomolecular archaeology of ancient tuberculosis: response to "Deficiencies and challenges in the study of ancient tuberculosis DNA" by Wilbur et al. *J. Archaeol. Sci*. 2009;36, 2797-804.

Donoghue HD, Lee OY, Minnikin DE, Besra GS, Taylor JH, Spigelman M. *Tuberculosis* in Dr Granville's mummy: a molecular re-examination of the earliest known Egyptian mummy to be scientifically examined and given a medical diagnosis. *Proc Biol Sci*. 2010;277(1678):51-6.

Drake RR, Cazare LH, Semmes OJ, Wadsworth JT. Serum, salivary and tissue proteomics for discovery of biomarkers for head and neck cancers. *Expert Rev Mol Diagn*. 2005;5(1):93-100.

Drancourt M, Aboudharam G, Signoli M, Dutour O, Raoult D. Detection of 400-year-old *Yersinia pestis* DNA in human dental pulp: an approach to the diagnosis of ancient septicemia. *Proc Natl Acad Sci U S A*. 1998;95(21):12637-40.

Edgar WM. Saliva: its secretion, composition and functions. *Br Dent J*. 1992;172(8):305-12.

Eng JK, McCormack AL, Yates JR. An approach to correlate tandem mass spectral data of peptides with amino acid sequences in a protein database. *J Am Soc Mass Spectrom*. 1994;5(11):976-89.

F Lam F, Jankova L, Dent OF, Molloy MP, Kwun SY, Clarke C, et al. Identification of distinctive protein expression patterns in colorectal adenoma. *Proteomics Clin Appl*. 2010;4(1):60-70.

Faerman M, Jankauskas R. Paleopathological and molecular evidence of human bone tuberculosis in Iron Age Lithuania. *Anthropol Anz*. 2000;58(1):57-62.

Feng J, Zhang X, Zhu H, Wang X, Ni S, Huang J. FoxQ1 overexpression influences poor prognosis in non-small cell lung cancer, associates with the phenomenon of EMT. *PLoS One*. 2012;7(6):e39937.

Fink-Puches R, Smolle J. Cytoskeleton and motility: an immunohistological and computer simulation analysis of melanocytic skin tumors. *J Cutan Pathol*. 1993;20(2):130-6.

Flores RJ, Li Y, Yu A, Shen J, Rao PH, Lau SS, et al. A systems biology approach reveals common metastatic pathways in osteosarcoma. *BMC Syst Biol*. 2012;6:50.

Folio C, Mora MI, Zalacain M, Corrales FJ, Segura V, Sierrasesúmaga L, et al. Proteomic analysis of chemo-naive pediatric osteosarcomas and corresponding normal bone reveals multiple altered molecular targets. *J Proteome Res*. 2009;8(8):3882-8.

Gerke V, Moss SE. Annexins: from structure to function. *Physiol Rev*. 2002;82(2):331-71.

Gernaey AM, Minnikin DE, Copley MS, Dixon RA, Middleton JC, Roberts CA. Mycolic acids and ancient DNA confirm an osteological diagnosis of tuberculosis. *Tuberculosis (Edinb)*. 2001;81(4):259-65.

Gerszten E, Allison MJ. Human soft tissue tumors in paleopathology. In: Ortner DJ, Aufderheide AC, eds. *Human paleopathology: current syntheses and future options*. Washington: Smithsonian Institution Press 1991.257–60.

Giarnieri E, De Vitis C, Noto A, Roscilli G, Salerno G, Mariotta S, et al. EMT markers in lung adenocarcinoma pleural effusion spheroid cells. *J Cell Physiol*. 2013;228(8):1720-6.

Gonsalves WC, Chi AC, Neville BW. Common oral lesions: Part II. Masses and neoplasia. *Am Fam Physician*. 2007;75(4):509-12.

Guan M, Tripathi V, Zhou X, Popescu NC. Adenovirus-mediated restoration of expression of the tumor suppressor gene DLC1 inhibits the proliferation and tumorigenicity of aggressive, androgen-independent human prostate cancer cell lines: prospects for gene therapy. *Cancer Gene Ther*. 2008;15(6):371-81.

Haas CJ, Zink A, Molnar E, Marcsik A, Dutour O, Nerlich A.G, et al. Molecular evidence for tuberculosis in Hungarian skeletal samples. In: Palfi Gy., Dutour, O., Deak, J., Hutas, I. (Eds), *Tuberculosis Past and Present*. Golden Book Publisher Ltd., Tuberculosis Foundation, Budapest-Szeged, 1999:385-95.

Haas CJ, Zink A, Molnár E, Szeimies U, Reischl U, Marcsik A, et al. Molecular evidence for different stages of tuberculosis in ancient bone samples from Hungary. *Am J Phys Anthropol*. 2000a;113(3):293-304.

Haas CJ, Zink A, Pálfi G, Szeimies U, Nerlich AG. Detection of leprosy in ancient human skeletal remains by molecular identification of *Mycobacterium leprae*. *Am J Clin Pathol*. 2000b;114(3):428-36.

Hao J, Wang K, Yue Y, Tian T, Xu A, Xiao X, et al. Selective expression of S100A11 in lung cancer and its role in regulating proliferation of adenocarcinomas cells. *Mol Cell Biochem*. 2012;359(1-2):323-32.

Hata H, Tatemichi M, Nakadate T. Involvement of annexin A8 in the properties of pancreatic cancer. *Mol Carcinog*. 2014;53(3):181-91.

Hendrix MJ, Seftor EA, Chu YW, Trevor KT, Seftor RE. Role of intermediate filaments in migration, invasion and metastasis. *Cancer Metastasis Rev*. 1996;15(4):507-25.

Hershkovitz I, Donoghue HD, Minnikin DE, Besra GS, Lee OY, Gernaey AM, et al. Detection and molecular characterization of 9,000-year-old *Mycobacterium tuberculosis* from a Neolithic settlement in the Eastern Mediterranean. *PLoS One*. 2008;3(10):e3426.

Hillenkamp F, Karas M, Ingeldoh A, Stahl B. Matrix assisted UV-laser desorption ionization: a new approach to mass spectrometry of large molecules, in Biological Mass Spectrometry, Elsevier, Amsterdam, 1990:49.

Hou F, Yuan W, Huang J, Qian L, Chen Z, Ge J, et al. Overexpression of EphA2 correlates with epithelial-mesenchymal transition-related proteins in gastric cancer and their prognostic importance for postoperative patients. Med Oncol. 2012;29(4):2691-700.

Hu S, Yu T, Xie Y, Yang Y, Li Y, Zhou X, et al. Discovery of oral fluid biomarkers for human oral cancer by mass spectrometry. Cancer Genomics Proteomics. 2007;4(2):55-64.

[http://www.uscnk.com/directory/Annexin-A10\(ANX-A10\)-4780.htm](http://www.uscnk.com/directory/Annexin-A10(ANX-A10)-4780.htm)

[http://www.uscnk.com/directory/BCL2-Related-Protein-A1\(BCL2A1\)-80252.htm](http://www.uscnk.com/directory/BCL2-Related-Protein-A1(BCL2A1)-80252.htm)

[http://www.uscnk.com/directory/Parkinson-Disease-7-Protein\(PARK7\)-80059.htm](http://www.uscnk.com/directory/Parkinson-Disease-7-Protein(PARK7)-80059.htm)

[http://www.uscnk.com/directory/Deleted-In-Liver-Cancer-\(DLC1\)-6500.htm](http://www.uscnk.com/directory/Deleted-In-Liver-Cancer-(DLC1)-6500.htm)

[http://www.uscnk.com/directory/Heat-Shock-Protein-B6-Alpha-Crystallin-Related\(HSPB6\)-5358.htm](http://www.uscnk.com/directory/Heat-Shock-Protein-B6-Alpha-Crystallin-Related(HSPB6)-5358.htm)

[http://www.uscnk.com/directory/S100-calcium-binding-protein-A11\(S100A11-S100C\)-0568.htm](http://www.uscnk.com/directory/S100-calcium-binding-protein-A11(S100A11-S100C)-0568.htm)

[http://www.uscnk.com/directory/Vimentin\(VIM\)-1040.htm](http://www.uscnk.com/directory/Vimentin(VIM)-1040.htm)

[http://elte.prompt.hu/sites/default/files/tananyagok/practical\\_biochemistry/ch07s03.html](http://elte.prompt.hu/sites/default/files/tananyagok/practical_biochemistry/ch07s03.html)

[http://www.premierbiosoft.com/tech\\_notes/mass-spectrometry.html](http://www.premierbiosoft.com/tech_notes/mass-spectrometry.html)

[http://www.giga.ulg.ac.be/jcms/cdu\\_15169/maldi-tof/tof-bruker-ultraflex-ii-tof/tof-april-2005](http://www.giga.ulg.ac.be/jcms/cdu_15169/maldi-tof/tof-bruker-ultraflex-ii-tof/tof-april-2005)

[http://www.matrixscience.com/help/fragmentation\\_help.html](http://www.matrixscience.com/help/fragmentation_help.html)

Jarai T, Maasz G, Burian A, Bona A, Jambor E, Gerlinger I, et al. Mass spectrometry-based salivary proteomics for the discovery of head and neck squamous cell carcinoma. *Pathol Oncol Res.* 2012;18(3):623-8.

Ji YF, Huang H, Jiang F, Ni RZ, Xiao MB. S100 family signaling network and related proteins in pancreatic cancer (Review). *Int J Mol Med.* 2014;33(4):769-76.

Jozsa L. *Paleopathologia.* Budapest: Semmelweis, 2006:74–5. (in Hungarian)

Kang JH, Park KK, Lee IS, Magae J, Ando K, Kim CH, et al. Proteome analysis of responses to ascochlorin in a human osteosarcoma cell line by 2-D gel electrophoresis and MALDI-TOF MS. *J Proteome Res.* 2006;5(10):2620-31.

Kang Y, Jung WY, Lee H, Jung W, Lee E, Shin BK, et al. Prognostic significance of heat shock protein 70 expression in early gastric carcinoma. *Korean J Pathol.* 2013;47(3):219-26.

Karas, M.; Bachmann, D.; Bahr, U.; Hillenkamp, F. Matrix-Assisted Ultraviolet Laser Desorption of Non-Volatile Compounds. *Int. J. Mass Spectrom. Ion Proc.* 1987;78:53-68

Karas M, Hillenkamp F. Laser desorption ionization of proteins with molecular masses exceeding 10,000 daltons. *Anal Chem.* 1988;60(20):2299-301.

Kelln EE, McMichael EV, Zimmermann B. A seventeenth century mandibular tumor in a North American Indian. *Oral Surg Oral Med Oral Pathol.* 1967;23(1):78-81.

Kim J, Kim MA, Jee CD, Jung EJ, Kim WH. Reduced expression and homozygous deletion of annexin A10 in gastric carcinoma. *Int J Cancer.* 2009;125(8):1842-50.

Kim JK, Kim PJ, Jung KH, Noh JH, Eun JW, Bae HJ, et al. Decreased expression of annexin A10 in gastric cancer and its overexpression in tumor cell growth suppression. *Oncol Rep.* 2010;24(3):607-12.

Kim LS, Kim JH. Heat shock protein as molecular targets for breast cancer therapeutics. *J Breast Cancer.* 2011;14(3):167-74.

Kim TY, Jong HS, Song SH, Dimtchev A, Jeong SJ, Lee JW, et al. Transcriptional silencing of the DLC-1 tumor suppressor gene by epigenetic mechanism in gastric cancer cells. *Oncogene*. 2003;22(25):3943-51.

Kim TY, Lee JW, Kim HP, Jong HS, Jung M, Bang YJ. DLC-1, a GTPase-activating protein for Rho, is associated with cell proliferation, morphology, and migration in human hepatocellular carcinoma. *Biochem Biophys Res Commun*. 2007;355(1):72-7.

Kim TY, Vigil D, Der CJ, Juliano RL. Role of DLC-1, a tumor suppressor protein with RhoGAP activity, in regulation of the cytoskeleton and cell motility. *Cancer Metastasis Rev*. 2009;28(1-2):77-83.

Kim TY, Jackson S, Xiong Y, Whitsett TG, Lobello JR, Weiss GJ, et al. CRL4A-FBXW5-mediated degradation of DLC1 Rho GTPase-activating protein tumor suppressor promotes non-small cell lung cancer cell growth. *Proc Natl Acad Sci U S A*. 2013;110(42):16868-73.

Kinsella RJ, Fitzpatrick DA, Creevey CJ, McInerney JO. Fatty acid biosynthesis in *Mycobacterium tuberculosis*: lateral gene transfer, adaptive evolution, and gene duplication. *Proc Natl Acad Sci U S A*. 2003;100(18):10320-5.

Knussmann R. *Anthropologie I*. Stuttgart, New York: Gustav Fischer, 1988:421–79.

Kolman CJ, Centurion-Lara A, Lukehart SA, Owsley DW, Tuross N. Identification of *Treponema pallidum* subspecies *pallidum* in a 200-year-old skeletal specimen. *J Infect Dis*. 1999;180(6):2060-3.

Kolman CJ, Tuross N. Ancient DNA analysis of human populations. *Am J Phys Anthropol*. 2000;111(1):5-23.

Kwon YJ, Jung JJ, Park NH, Ye DJ, Kim D, Moon A, et al. Annexin a5 as a new potential biomarker for Cisplatin-induced toxicity in human kidney epithelial cells. *Biomol Ther (Seoul)*. 2013;21(3):190-5.

Lehtinen L, Ketola K, Mäkelä R, Mpindi JP, Viitala M, Kallioniemi O, et al. High-throughput RNAi screening for novel modulators of vimentin expression identifies MTHFD2 as a regulator of breast cancer cell migration and invasion. *Oncotarget*. 2013;4(1):48-63.

Li G, Zhang W, Zeng H, Chen L, Wang W, Liu J, et al. An integrative multi-platform analysis for discovering biomarkers of osteosarcoma. *BMC Cancer*. 2009;9:150.

Li G, Cai M, Fu D, Chen K, Sun M, Cai Z, et al. Heat shock protein 90B1 plays an oncogenic role and is a target of microRNA-223 in human osteosarcoma. *Cell Physiol Biochem*. 2012;30(6):1481-90.

Li M, Zhao ZW, Zhang Y, Xin Y. Over-expression of Ephb4 is associated with carcinogenesis of gastric cancer. *Dig Dis Sci*. 2011;56(3):698-706.

Li N, Long Y, Fan X, Liu H, Li C, Chen L, et al. Proteomic analysis of differentially expressed proteins in hepatitis B virus-related hepatocellular carcinoma tissues. *J Exp Clin Cancer Res*. 2009;28:122.

Li Y, Liang Q, Wen YQ, Chen LL, Wang LT, Liu YL, et al. Comparative proteomics analysis of human osteosarcomas and benign tumor of bone. *Cancer Genet Cytogenet*. 2010;198(2):97-106.

Lin LL, Huang HC, Juan HF. Revealing the molecular mechanism of gastric cancer marker annexin A4 in cancer cell proliferation using exon arrays. *PLoS One*. 2012;7(9):e44615.

Liu H, Wang M, Li M, Wang D, Rao Q, Wang Y, et al. Expression and role of DJ-1 in leukemia. *Biochem Biophys Res Commun*. 2008;375(3):477-83.

Liu SH, Lin CY, Peng SY, Jeng YM, Pan HW, Lai PL, et al. Down-regulation of annexin A10 in hepatocellular carcinoma is associated with vascular invasion, early recurrence, and poor prognosis in synergy with p53 mutation. *Am J Pathol*. 2002;160(5):1831-7.

Liu XG, Wang XP, Li WF, Yang S, Zhou X, Li SJ, et al. Ca<sup>2+</sup>-binding protein S100A11: a novel diagnostic marker for breast carcinoma. *Oncol Rep*. 2010;23(5):1301-8.

Luo M, Hajjar KA. Annexin A2 system in human biology: cell surface and beyond. *Semin Thromb Hemost*. 2013;39(4):338-46.

Macht M, Asperger A, Deininger SO. Comparison of laser-induced dissociation and high-energy collision-induced dissociation using matrix-assisted laser

desorption/ionization tandem time-of-flight (MALDI-TOF/TOF) for peptide and protein identification. *Rapid Commun Mass Spectrom.* 2004;18(18):2093-105.

Maczel M. "On the traces of tuberculosis" diagnostic criteria of tuberculous affection of the human skeleton and their application in Hungarian and French anthropological series. Phd thesis. University of la Méditerranée aix Marseille II Faculty of Medicine. Marseille. Department of Anthropology. University of Szeged, 2003.

Mahadevan D, Spier C, Della Croce K, Miller S, George B, Riley C, et al. Transcript profiling in peripheral T-cell lymphoma, not otherwise specified, and diffuse large B-cell lymphoma identifies distinct tumor profile signatures. *Mol Cancer Ther.* 2005;4(12):1867-79.

Mamyrin BA, Karataev VI, Schmikk DB, Zagulin BA. The massreflectron, a new nonmagnetic time-offlight mass spectrometer with high resolution. *Sov. Phys. JETP* 1973;37:45–8.

Marcsik A., Palfi G. Data for the epidemiology of skeletal tuberculosis in ancient populations. *Człowiek w czasie i przestrzeni*, Gdańsk, 1993:354-58.

Marinova DM, Slavova YG, Trifonova N, Kostadinov D, Maksimov V, Petrov D. Stress protein Hsp27 expression predicts the outcome in operated small cell lung carcinoma and large cell neuroendocrine carcinoma patients. *J BUON.* 2013;18(4):915-20.

Mark L. Csontmaradványok mycobacteriális fertőzésének meghatározása tömegspektrometriával. *Folia Antropol.* 2007;5:45-50.

Mark L, Patonai Z, Vaczy A, Lorand T, Marcsik A. High-throughput mass spectrometric analysis of 1400-year-old mycolic acids as biomarkers for ancient tuberculosis infection. *J. Archaeol. Sci.* 2010;37:302-5.

Mark L, Gulyas-Fekete G, Marcsik A, Molnar E, Palfi G. Analysis of ancient mycolic acids by using MALDI TOF MS: response to "Essentials in the use of mycolic acid biomarkers for tuberculosis detection" by Minnikin et al., 2010. *J. Archaeol. Sci* 2011;38:1111-8.

Marocchio LS, Lima J, Sperandio FF, Corrêa L, de Sousa SO. Oral squamous cell carcinoma: an analysis of 1,564 cases showing advances in early detection. *J Oral Sci.* 2010;52(2):267-73.

Mathema B, Kurepina NE, Bifani PJ, Kreiswirth BN. Molecular epidemiology of tuberculosis: current insights. *Clin Microbiol Rev.* 2006;19(4):658-85.

Matthiesen R. *Mass Spectrometry Data Analysis in Proteomics.* Humana Press, Totowa, New Jersey. 2007;89.

Mays S, Taylor GM, Legge AJ, Young DB, Turner-Walker G. Paleopathological and biomolecular study of tuberculosis in a medieval skeletal collection from England. *Am J Phys Anthropol.* 2001;114(4):298-311.

Mays S, Taylor GM. A first prehistoric case of tuberculosis from Britain. *Intern. J. Osteoarchaeol.* 2003;13:189–96.

McKiernan E, McDermott EW, Evoy D, Crown J, Duffy MJ. The role of S100 genes in breast cancer progression. *Tumour Biol.* 2011;32(3):441-50.

McLuckey SA. Principles of collisional activation in analytical mass spectrometry. *J Am Soc Mass Spectrom.* 1992;3(6):599-614.

Melle C, Ernst G, Schimmel B, Bleul A, Mothes H, Kaufmann R, et al. Different expression of calgizzarin (S100A11) in normal colonic epithelium, adenoma and colorectal carcinoma. *Int J Oncol.* 2006;28(1):195-200.

Merikallio H, Pääkkö P, Kinnula VL, Harju T, Soini Y. Nuclear factor erythroid-derived 2-like 2 (Nrf2) and DJ1 are prognostic factors in lung cancer. *Hum Pathol.* 2012;43(4):577-84.

Minnikin DE, Lee OY, Pitts M, Baird MS, Besra GS. Essentials in the use of mycolic acid biomarkers for tuberculosis detection: response to “High-throughput mass spectrometric analysis of 1400-year-old mycolic acids as biomarkers for ancient tuberculosis infection” by Mark et al., 2010. *J. Archaeol. Sci* 2010;37: 2407-12.

Mogami T, Yokota N, Asai-Sato M, Yamada R, Koizume S, Sakuma Y, et al. Annexin A4 is involved in proliferation, chemo-resistance and migration and invasion in ovarian clear cell adenocarcinoma cells. *PLoS One.* 2013;8(11):e80359.

Molnar E, Palfi G. Probable cases of skeletal infections in the 17<sup>th</sup> century anthropological series from Bacsalmas (Hungary). *Acta Biol. Szeged.* 1994;40:117-32.

Molnar E, Maczel M, Marcsik A, Palfi G, Nerlich GA, Zink A. A csont-ízületi tuberculosis molekuláris vizsgálata egy középkori temető embertani anyagában. *Folia Anthropol.* 2005;3:41-51.

Montiel R, García C, Cañadas MP, Isidro A, Guijo JM, Malgosa A. DNA sequences of *Mycobacterium leprae* recovered from ancient bones. *FEMS Microbiol Lett.* 2003;226(2):413-4.

Mori M, Shimada H, Gunji Y, Matsubara H, Hayashi H, Nimura Y, et al. S100A11 gene identified by in-house cDNA microarray as an accurate predictor of lymph node metastases of gastric cancer. *Oncol Rep.* 2004;11(6):1287-93.

Munksgaard PP, Mansilla F, Brems Eskildsen AS, Frstrup N, Birkenkamp-Demtröder K, Uihøi BP, et al. Low ANXA10 expression is associated with disease aggressiveness in bladder cancer. *Br J Cancer.* 2011;105(9):1379-87.

Nagy B, Lundán T, Larramendy ML, Aalto Y, Zhu Y, Niini T, et al. Abnormal expression of apoptosis-related genes in haematological malignancies: overexpression of MYC is poor prognostic sign in mantle cell lymphoma. *Br J Haematol.* 2003;120(3):434-41.

Nielsen-Marsh CM, Richards MP, Hauschka PV, Thomas-Oates JE, Trinkaus E, Pettitt PB, et al. Osteocalcin protein sequences of Neanderthals and modern primates. *Proc Natl Acad Sci U S A.* 2005;102(12):4409-13.

Nielsen-Marsh CM, Stegemann C, Hoffmann R, Smith T, Feeney R, Toussaint M, et al. Extraction and sequencing of human and Neanderthal mature enamel proteins using MALDI-TOF/TOF MS. *J. Archaeol. Sci.* 2009;36:1758-63.

Niforou KM, Anagnostopoulos AK, Vougas K, Kittas C, Gorgoulis VG, Tsangaris GT. The proteome profile of the human osteosarcoma U2OS cell line. *Cancer Genomics Proteomics.* 2008;5(1):63-78.

Noguchi T, Sato T, Takeno S, Uchida Y, Kashima K, Yokoyama S, et al. Biological analysis of gastrointestinal stromal tumors. *Oncol Rep.* 2002;9(6):1277-82.

Ohuchida K, Mizumoto K, Ohhashi S, Yamaguchi H, Konomi H, Nagai E, et al. S100A11, a putative tumor suppressor gene, is overexpressed in pancreatic carcinogenesis. *Clin Cancer Res.* 2006;12(18):5417-22.

Olsen JV, Ong SE, Mann M. Trypsin cleaves exclusively C-terminal to arginine and lysine residues. *Mol. Cell Proteomics* 2004;3:608–14.

Orlando LAA, Ginolhac A, Zhang G, Froese D, Albrechtsen A et al. Recalibrating Equus evolution using the genome sequence of an early Middle Pleistocene horse. *Nature* 2013;499(7456):74-8.

Ostrom PH, Gandhi H, Strahler JR, Walker AK, Andrews PC, Leykam J, et al.. Unraveling the sequence and structure of the protein osteocalcin from a 42 ka fossil horse. *Geochim. Cosmochim. Acta* 2006;70:2034-44.

Ottina E, Tischner D, Herold MJ, Villunger A. A1/Bfl-1 in leukocyte development and cell death. *Exp Cell Res.* 2012;318(11):1291-303.

Oue N, Hamai Y, Mitani Y, Matsumura S, Oshimo Y, Aung PP, et al. Gene expression profile of gastric carcinoma: identification of genes and tags potentially involved in invasion, metastasis, and carcinogenesis by serial analysis of gene expression. *Cancer Res.* 2004;64(7):2397-405.

Palfi G. The osteo-archaeological evidence of vertebral tuberculosis in the 8th century. *Acta Biol. Szeged.* 1991;37:101-5.

Palfi G, Molnar E. The Paleopathology of specific infectious diseases from Southeastern Hungary: a brief overview. *Acta Biol. Szeged.* 2009;53:111-6.

Peng H, Long F, Wu Z, Chu Y, Li J, Kuai R, et al. Downregulation of DLC-1 gene by promoter methylation during primary colorectal cancer progression. *Biomed Res Int.* 2013;2013:181384.

Peng SY, Ou YH, Chen WJ, Li HY, Liu SH, Pan HW, et al. Aberrant expressions of annexin A10 short isoform, osteopontin and alpha-fetoprotein at chromosome 4q

cooperatively contribute to progression and poor prognosis of hepatocellular carcinoma. *Int J Oncol*. 2005;26(4):1053-61.

Perkins DN, Pappin DJ, Creasy DM, Cottrell JS. Probability-based protein identification by searching sequence databases using mass spectrometry data. *Electrophoresis*. 1999;20(18):3551-67.

Plaumann M, Seitz S, Frege R, Estevez-Schwarz L, Scherneck S. Analysis of DLC-1 expression in human breast cancer. *J Cancer Res Clin Oncol*. 2003;129(6):349-54.

Pruitt KD, Tatusova T, Maglott DR. NCBI Reference Sequence (RefSeq): a curated non-redundant sequence database of genomes, transcripts and proteins. *Nucleic Acids Res*. 2005;33(Database issue):D501-4.

Qin Y, Chu B, Gong W, Wang J, Tang Z, Shen J, et al. The inhibitory effects of deleted in liver cancer 1 gene on gallbladder cancer growth through induction of cell cycle arrest and apoptosis. *J Gastroenterol Hepatol*. 2014;29(5):964-72.

Rafi A, Spigelman M, Stanford J, Lemma E, Donoghue H, Zias J. *Mycobacterium leprae* DNA from ancient bone detected by PCR. *Lancet*. 1994;343(8909):1360-1.

Raoult D, Aboudharam G, Crubézy E, Larrouy G, Ludes B, Drancourt M. Molecular identification by "suicide PCR" of *Yersinia pestis* as the agent of medieval black death. *Proc Natl Acad Sci U S A*. 2000;97(23):12800-3.

Rehman I, Azzouzi AR, Cross SS, Deloulme JC, Catto JW, Wylde N, et al. Dysregulated expression of S100A11 (calgizzarin) in prostate cancer and precursor lesions. *Hum Pathol*. 2004;35(11):1385-91.

Riker AI, Enkemann SA, Fodstad O, Liu S, Ren S, Morris C, et al. The gene expression profiles of primary and metastatic melanoma yields a transition point of tumor progression and metastasis. *BMC Med Genomics*. 2008;1:13.

Rodrigues MM, Rema A, Gärtner F, Soares FA, Rogatto SR, De Mour VM, et al. Overexpression of vimentin in canine prostatic carcinoma. *J Comp Pathol*. 2011;144(4):308-11.

Roesch-Ely M, Nees M, Karsai S, Ruess A, Bogumil R, Warnken U, et al. Proteomic analysis reveals successive aberrations in protein expression from healthy mucosa to invasive head and neck cancer. *Oncogene*. 2007;26(1):54-64.

Rothschild BM, Martin LD, Lev G, Bercovier H, Bar-Gal GK, Greenblatt C, et al. *Mycobacterium tuberculosis* complex DNA from an extinct bison dated 17,000 years before the present. *Clin Infect Dis*. 2001;33(3):305-11.

Ruffer M, Willmore J. Note on a tumor of the pelvis dated from Roman time (250 AD) and found in Egypt. *Journal of Pathology and Bacteriology*. 1914;18:480–4.

Salama I, Malone PS, Mihaimeed F, Jones JL. A review of the S100 proteins in cancer. *Eur J Surg Oncol*. 2008;34(4):357-64.

Saleh A, Zain RB, Hussaini H, Ng F, Tanavde V, Hamid S, et al. Transcriptional profiling of oral squamous cell carcinoma using formalin-fixed paraffin-embedded samples. *Oral Oncol*. 2010;46(5):379-86.

Sallares R, Gomzi S. Biomolecular archaeology of malaria. *Ancient Biomol*. 2001;3:195-213.

Satelli A, Li S. Vimentin in cancer and its potential as a molecular target for cancer therapy. *Cell Mol Life Sci*. 2011;68(18):3033-46.

Schultz M, Parzinger H, Posdnjakov DV, Chikisheva TA, Schmidt-Schultz TH. Oldest known case of metastasizing prostate carcinoma diagnosed in the skeleton of a 2,700-year-old Scythian king from Arzhan (Siberia, Russia). *Int J Cancer*. 2007;121(12):2591-5.

Shimizu T, Kasamatsu A, Yamamoto A, Koike K, Ishige S, Takatori H, et al. Annexin A10 in human oral cancer: biomarker for tumoral growth via G1/S transition by targeting MAPK signaling pathways. *PLoS One*. 2012;7(9):e45510.

Shukla AK, Futrell JH. Tandem mass spectrometry: dissociation of ions by collisional activation. *J Mass Spectrom*. 2000;35(9):1069-90.

Singh S, Sadacharan S, Su S, Belldegrun A, Persad S, Singh G. Overexpression of vimentin: role in the invasive phenotype in an androgen-independent model of prostate cancer. *Cancer Res*. 2003;63(9):2306-11.

Sitaram RT, Cairney CJ, Grabowski P, Keith WN, Hallberg B, Ljungberg B, et al. The PTEN regulator DJ-1 is associated with hTERT expression in clear cell renal cell carcinoma. *Int J Cancer*. 2009;125(4):783-90.

Sjoestroem C, Khosravi S, Cheng Y, Safaee Ardekani G, Martinka M, Li G. DLC1 expression is reduced in human cutaneous melanoma and correlates with patient survival. *Mod Pathol*. 2014;27(9):1203-11.

Smith I. *Mycobacterium tuberculosis* pathogenesis and molecular determinants of virulence. *Clin Microbiol Rev*. 2003;16(3):463-96.

Spengler B, Kirsch D, Kaufmann R. Metastable decay of peptides and proteins in matrix assisted laser desorption mass spectrometry. *Rapid Commun. Mass Spectrom*. 1991;5:198–202.

Stephens, WE. A Pulsed Mass Spectrometer With Time Dispersion. *Phys. Rev*. 1946;69:691.

Stone AC, Wilbur AK, Buikstra JE, Roberts CA. Tuberculosis and leprosy in perspective. *Am J Phys Anthropol*. 2009;140 Suppl 49:66-94.

Strouhal E, Vyhnánek L, Horácková L, Benesová L, Nemečková A. Malignant tumors affecting the people from the ossuary at Krtiny (Czech Republic). *Journal of Paleopathology* 1996;8:5–24.

Stump MJ, Fleming RC, Gong WH, Jaber AJ, Jones JJ, Surber CW et al. Matrix-Assisted Laser Desorption Mass Spectrometry. *Appl. Spectrosc. Rev*. 2002;37:275-303.

Suckau D, Resemann A, Schuerenberg M, Hufnagel P, Franzen J, Holle A. A novel MALDI LIFT-TOF/TOF mass spectrometer for proteomics. *Anal Bioanal Chem*. 2003;376(7):952-65.

Suehara Y, Kubota D, Kikuta K, Kaneko K, Kawai A, Kondo T. Discovery of biomarkers for osteosarcoma by proteomics approaches. *Sarcoma*. 2012;2012:425636.

Sun MY, Xing RH, Gao XJ, Yu X, He HM, Gao N, et al. ANXA2 regulates the behavior of SGC-7901 cells. *Asian Pac J Cancer Prev*. 2013;14(10):6007-12.

Suzuki T. Paleopathological study on a case of osteosarcoma. *Am J Phys Anthropol.* 1987;74(3):309-18.

Szanto I, Mark L, Bona A, Maasz G, Sandor B, Gelencser G, et al. High-throughput screening of saliva for early detection of oral cancer: a pilot study. *Technol Cancer Res Treat.* 2012;11(2):181-8.

Tanaka K; Waki H; Ido Y; Akita S; Yoshida Y; Yhoshida T. Protein and Polymer Analyses Up to M/z 100,000 by Laser Ionization Time-of-Flight Mass Spectrometry. *Rapid Commun. Mass Spectrom.* 1988;2:151-3.

Tanaka M, Adzuma K, Iwami M, Yoshimoto K, Monden Y, Itakura M. Human calgizzarin; one colorectal cancer-related gene selected by a large scale random cDNA sequencing and northern blot analysis. *Cancer Lett.* 1995;89(2):195-200.

Tauler J, Zudaire E, Liu H, Shih J, Mulshine JL. hnRNP A2/B1 modulates epithelial-mesenchymal transition in lung cancer cell lines. *Cancer Res.* 2010;70(18):7137-47.

Taylor MG, Rutland P, Molleson T. A sensitive polymerase chain reaction method for the detection of *Plasmodium* species DNA in ancient human remains. *Ancient Biomol.* 1997;1:193-203.

Taylor MG, Goyal M, Legge AJ, Shaw RJ, Young D. Genotypic analysis of *Mycobacterium tuberculosis* from medieval human remains. *Microbiology.* 1999;145:899-904.

Taylor MG, Widdison S, Brown IN, Young D. A mediaeval case of lepromatous leprosy from 13-14<sup>th</sup> century Orkney, Scotland. *J. Archaeol. Sci.* 2000;27:1113-38.

Taylor MG, Murphy E, Hopkins R, Rutland P, Chistov Y. First report of *Mycobacterium bovis* DNA in human remains from the Iron Age. *Microbiol.* 2007;153:1243-49.

Taylor MG, Blau S, Mays S, Monot M, Lee OY, Minnikin DE, et al. *Mycobacterium leprae* genotype amplified from an archaeological case of lepromatous leprosy in Central Asia. *J. Archaeol. Sci.* 2009;36:2408-14.

Tian M, Cui YZ, Song GH, Zong MJ, Zhou XY, Chen Y, et al. Proteomic analysis identifies MMP-9, DJ-1 and A1BG as overexpressed proteins in pancreatic juice from pancreatic ductal adenocarcinoma patients. *BMC Cancer*. 2008;8:241.

Tian T, Hao J, Xu A, Luo C, Liu C, Huang L, et al. Determination of metastasis-associated proteins in non-small cell lung cancer by comparative proteomic analysis. *Cancer Sci*. 2007;98(8):1265-74.

Ullmannova-Benson V, Guan M, Zhou X, Tripathi V, Yang XY, Zimonjic DB, et al. DLC1 tumor suppressor gene inhibits migration and invasion of multiple myeloma cells through RhoA GTPase pathway. *Leukemia*. 2009;23(2):383-90.

Vogler M. BCL2A1: the underdog in the BCL2 family. *Cell Death Differ*. 2012;19(1):67-74.

Wang C, Zhang Z, Li L, Zhang J, Wang J, Fan J, et al. S100A11 is a migration-related protein in laryngeal squamous cell carcinoma. *Int J Med Sci*. 2013;10(11):1552-9.

Wang G, Wang X, Wang S, Song H, Sun H, Yuan W, et al. Colorectal cancer progression correlates with upregulation of S100A11 expression in tumor tissues. *Int J Colorectal Dis*. 2008;23(7):675-82.

Wei J, Xu G, Wu M, Zhang Y, Li Q, Liu P, et al. Overexpression of vimentin contributes to prostate cancer invasion and metastasis via src regulation. *Anticancer Res*. 2008;28(1A):327-34.

Weinberg MA, Estefan DJ. Assessing oral malignancies. *Am Fam Physician*. 2002;65:1379-84.

Wilbur AK, Bouwman AS, Stone AC, Roberts CA, Pfister LA, Buikstra JE, et al. Deficiencies and challenges in the study of ancient tuberculosis DNA. *J. Archaeol. Sci*. 2009;36:1990-7.

Willimott S, Wagner SD. miR-125b and miR-155 contribute to BCL2 repression and proliferation in response to CD40 ligand (CD154) in human leukemic B-cells. *J Biol Chem*. 2012;287(4):2608-17.

Wolosz D, Walczak A, Wilczynski GM, Szparecki G, Wilczek E, Gornicka B. Deleted in liver cancer 1 expression and localization in hepatocellular carcinoma tissue sections. *Oncol Lett.* 2014;8(2):785-8. doi: 10.3892/ol.2014.2216.

Xiao MB, Jiang F, Ni WK, Chen BY, Lu CH, Li XY, et al. High expression of S100A11 in pancreatic adenocarcinoma is an unfavorable prognostic marker. *Med Oncol.* 2012;29(3):1886-91.

Yajima T, Ochiai H, Uchiyama T, Takano N, Shibahara T, Azuma T. Resistance to cytotoxic chemotherapy-induced apoptosis in side population cells of human oral squamous cell carcinoma cell line Ho-1-N-1. *Int J Oncol.* 2009;35(2):273-80.

Yang X, Popescu NC, Zimonjic DB. DLC1 interaction with S100A10 mediates inhibition of in vitro cell invasion and tumorigenicity of lung cancer cells through a RhoGAP-independent mechanism. *Cancer Res.* 2011;71(8):2916-25.

Yao R, Davidson DD, Lopez-Beltran A, MacLennan GT, Montironi R, Cheng L. The S100 proteins for screening and prognostic grading of bladder cancer. *Histol Histopathol.* 2007;22(9):1025-32.

Yuan BZ, Jefferson AM, Baldwin KT, Thorgeirsson SS, Popescu NC, Reynolds SH. DLC-1 operates as a tumor suppressor gene in human non-small cell lung carcinomas. *Oncogene.* 2004;23(7):1405-11.

Zamay TN, Kolovskaya OS, Glazyrin YE, Zamay GS, Kuznetsova SA, Spivak EA, et al. DNA-aptamer targeting vimentin for tumor therapy in vivo. *Nucleic Acid Ther.* 2014;24(2):160-70.

Zeng C, Ke Z, Song Y, Yao Y, Hu X, Zhang M, et al. Annexin A3 is associated with a poor prognosis in breast cancer and participates in the modulation of apoptosis in vitro by affecting the Bcl-2/Bax balance. *Exp Mol Pathol.* 2013;95(1):23-31.

Zhang T, Zheng J, Jiang N, Wang G, Shi Q, Liu C, et al. Overexpression of DLC-1 induces cell apoptosis and proliferation inhibition in the renal cell carcinoma. *Cancer Lett.* 2009;283(1):59-67.

Zhao CH, Li QF, Zhao Y, Niu JW, Li ZX, Chen JA. Changes of nuclear matrix proteins following the differentiation of human osteosarcoma MG-63 cells. *Genomics Proteomics Bioinformatics*. 2006;4(1):10-7.

Zhu XL, Wang ZF, Lei WB, Zhuang HW, Jiang HY, Wen WP. DJ-1: a novel independent prognostic marker for survival in glottic squamous cell carcinoma. *Cancer Sci*. 2010;101(5):1320-5.

Zink A, Haas CJ, Reischl U, Szeimies U, Nerlich AG. Molecular analysis of skeletal tuberculosis in an ancient Egyptian population. *J Med Microbiol*. 2001;50(4):355-66.

## 10. List of Publications

*This work is based on the following articles:*

1. **Bona A**, Papai Z, Maasz G, Toth GA, Jambor E, Schmidt J, et al. Mass spectrometric identification of ancient proteins as potential molecular biomarkers for a 2000-year-old osteogenic sarcoma. PLoS One. 2014;9(1):e87215.

**Impact factor: 3.534**

**Citation: 0**

2. Boros-Major A, **Bona A**, Lovasz G, Molnar E, Marcsik A, et al. New perspectives in biomolecular paleopathology of ancient tuberculosis: a proteomic approach. J. Archaeol. Sci. 2011;38:197–201.

**Impact factor: 1.914**

**Citation: 8**

*Further publications:*

Budán Ferenc, Szabó István, Jámbor Éva, **Bóna Ágnes**, Váczy Alexandra, Maász Gábor, Ohmacht Róbert, Kiss István, Márk László, Tényi Tamás: A skizofrénia biomarkereinek kimutatása és azonosítása tömegspektrometriával új lehetőséget nyithat a megelőzésben. Magyar Epidemiológia 7: p. 69. (2010)

Jarai T., Maasz G., Burian A., **Bona A.**, Jambor E., Gerlinger I., Mark L.: Mass spectrometry-based salivary proteomics for the discovery of head and neck squamous cell carcinoma, Pathol. Oncol. Res. 18(3): 623-628 (2012)

**Impact factor: 1.555**

**Citation: 18**

Szabó Gy. T.; Tihanyi R.; Csulak F.; Jámbor É.; **Bóna Á.**; Szabó Gy.; Márk L.: Comparative salivary proteomics of cleft palate patients, *The Cleft Palate-Craniofacial Journal* 49(5): 519-523 (2012)

**Impact factor: 1.238**

**Citation: 4**

Szántó I., Márk L., **Bóna Á.**, Maász G., Sándor B., Gelencsér G., Túri Zs., Gallyas F.: High-throughput screening of saliva for early detection of oral cancer.: A pilot study, *Technology in Cancer Research and Treatment* 11(2): 181-188. (2012)

**Impact factor: 1.943**

**Citation: 9**

Gubicskóné Kisbenedek Andrea; Kovács Bernadett; Polyák Éva; Szekeresné Szabó Szilvia; Breitenbach Zita; Szabó Zoltán; Márk László; **Bóna Ágnes**; Figler Mária: A bogyós gyümölcsökből készült készítmények Rezveratrol-, rutin- és kvercetin tartalmának meghatározása Új Diéta. - ISSN 1587-169X. - 2012. 19. évf. 5-6. sz., p. 34-35.

Eva Jambor, **Agnes Bona**, Janos Schmidt, Laszlo Mark, Robert Ohmacht: Preparation and investigation of LC packing made by microwave-assisted solid-phase synthesis. *Journal of Separation Science* 36 (5) 827–831 (2013)

**Impact factor: 2.594**

**Citation: 0**

Kisbenedek G. A., Szabó Sz., Polyák É., Breitenbach Z., **Bóna Á.**, Márk L., Figler M.: Analysis of trans-resveratrol in oilseeds by high performance liquid chromatography, *Acta Alimentaria* (2013)

**Impact factor: 0.427**

**Citation: 0**

**Total impact factor: 13.205**

**Total citations: 39**

## Abstracts:

Wölfling J, **Bóna Á**, Frank É, Schneider Gy, Berényi Á, Zupkó I: Synthesis and cytotoxic activity of 16-benzylidene estrone 3-methyl ethers. Hungarian-Austrian-Czech-German-Greek-Italian-Polish-Slovak-Slovenian Joint Meeting on Medicinal Chemistry, Budapest, Hungary, June 24-27, 2009.

E. Jambor, **A. Bona**, B. Sümegi, L. Mark: Proteomic analysis of intracellular targets for BGP-15. 3rd Central and Eastern European Proteomics Conference, Budapest, Hungary, October 6-9, 2009.

**A. Bona**, G. Maasz, E. Jambor, G. Montsko, R. Ohmacht, L. Mark: Quantitative analysis of steroid hormones by fullerene-assisted laser desorption/ionization MS. 28th Informal Meeting on Mass Spectrometry, Kőszeg, Hungary, May 2-6, 2010.

Gabor Maasz, **Agnes Bona**, Eva Jambor, Gergely Montsko, Robert Ohmacht, Laszlo Mark: Determination of steroid hormones by MALDI TOF MS with using fullerene as the matrix. 40. Membrán-transzport konferencia, Sümeg, Május 18-21, 2010.

**Bona A.**; Boros Major A.; Maasz G.; Jambor E.; Mark L.: LC-MS identification of mycolic acids and their metabolites as biomarkers for ancient tuberculosis 28th International Symposium on Chromatography, Valencia, September 12-16, 2010.

Jambor E.; Patko B.; **Bona A.**; Maasz G.; Mark L.; Ohmacht R.: Quantitative detection of carcinoid tumor markers by HPLC–MS. 28th International Symposium on Chromatography, Valencia, September 12-16, 2010.

Boros Major A., **Bona A.**, Jambor E., Montsko G., Ohmacht R., Mark L.: Trans-resveratrol and trans-piceid in hungarian wines. 28th International Symposium on Chromatography, Valencia, September 12-16, 2010.

**Bóna Á.**, Maász G., Pirger Zs., Lubics A., Reglódi D., László Z., Kiss T., Márk L.: Neuropeptid profil vizsgálata csigákban (Helix pomatia) MS segítségével. Elválasztástudományi Vándorgyűlés, Tapolca, 2010.november 10-12.

**Agnes Bona** , Eva Jambor , Gabor Maasz , Robert Ohmacht , Laszlo Mark: Mass spectrometry based analysis of TDPA - a novel naturally occurring stilbene derivative in Hungarian wines, 29th Informal Meeting on Mass Spectrometry, Fiera di Primiero, Italy, May 15-19, 2011.

Gabor Maasz, Eva Jambor, **Agnes Bona**, Aniko Takatsy, Laszlo Mark: Quantitative LC-MS based analysis of Somatostatin in clinical samples, 29 th Informal Meeting on Mass Spectrometry, Fiera di Primiero, Italy, May 15-19, 2011.

**Agnes Bona**, Zsolt Pirger, Gabor Maasz, Eva Jambor, Zita Laszto, Mark Laszlo: Three-Dimensional, High Resolution MALDI MS Imaging Investigation of Neuropeptides in the Pond Snail, Lymnaea Stagnalis. Pittcon 2012 Conference and Expo, Orlando, Florida, March 11-15, 2012.

Éva Jámbor, **Ágnes Bóna**, László Márk, Róbert Ohmacht: Stationary Phase Made by Solid Phase Synthesis. HPLC 2011, Budapest, Hungary, June 19-23, 2011.

Gubicskóné Kisbenedek Andrea, Szabó Szilvia, Polyák Éva, Bonyárné Müller Katalin, Kovács Bernadett, **Bóna Ágnes**, Márk László, Figler Mária: Bogyós gyümölcskészítmények polifenol tartalmának meghatározása. Magyar Gasztroenterológiai Társaság 54. nagygyűlése, Tihany, 2012.06.02-2012.06.05.

Gubicskóné Kisbenedek Andrea, Szabó Szilvia, Kovács Bernadett, Bonyárné Müller Katalin, **Bóna Ágnes**, Márk László, Figler Mária: Bogyós gyümölcsökből készült termékek polifenol tartalmának meghatározása. A Magyar Táplálkozástudományi Társaság 37. vándorgyűlése, Balatonőszöd, 2012.10.04-2012.10.06.

Jámbor Éva, **Bóna Ágnes**, Schmidt János, Márk László, Ohmacht Róbert: Folyadékkromatográfiás töltetek előállítása mikrohullámú szintézissel. Elválasztástudományi Vándorgyűlés, Hajduszoboszló, 2012. november 7-9.

Zoltan Papai, **Agnes Bona**, Gabor Maasz, Janos Schmidt, Robert Ohmacht, Laszlo Mark: Investigation of trans-resveratrol and stilbene derivative TDPA in hungarian wines using HPLC and LC-MS. Chemical Reactions in Food VII, Prague, Czech Republic November 14-16, 2012.

Zoltan Papai, Gabor Maasz, Janos Schmidt, **Agnes Bona**, Katalin Böddi, Dora Petrovics, Laszlo Mark: nHPLC-MS determination of DA and DA metabolites in mouse brain. 31th Informal Meeting on Mass Spectrometry, Palermo, Italy May 5-8, 2013.

**Agnes Bona**, Dora Petrovics, Katalin Boddi, Eva Jambor, Gabor Maasz, Akos Varnagy, Janos Schmidt, Jozsef Bodis, Laszlo Mark: Mass spectrometry-based screening for prediction of embryo viability. 9th Balaton Symposium on High-Performance Separation Methods, Siófok, Hungary, September 4-6, 2013.

**Agnes Bona**, Zoltan Papai, Eva Jambor, Gabor Maasz, Janos Schmidt, Laszlo Mark:  
Analysis of paleopathological remains using MALDI TOF/TOF MS. 32nd Informal  
Meeting on Mass Spectrometry, Balatonszárszó, Hungary, May 11-14, 2014.

## Presentations:

Jámbor Éva, **Bóna Ágnes**, Váczy Alexandra, Maász Gábor, Ohmacht Róbert, Tényi Tamás, Márk László: Patológias biomarkerek kimutatása és azonosítása tömegspektrometriával. Biológus Doktoranduszok Konferenciája, PAB Székház, 2009. november 12-13.

Budán Ferenc, Szabó István, Jámbor Éva, **Bóna Ágnes**, Váczy Alexandra, Maász Gábor, Ohmacht Robert, Kiss István, Márk László, Tényi Tamás: A skizofrénia biomarkereinek kimutatása és azonosítása tömegspektrometriával új lehetőségeket nyithat a megelőzésben, Népegészségügyi Tudományos Társaság XVIII. Nemzetközi Kongresszusa Orosháza-Gyopárosfürdő, 2010.május 13-15.

Maász Gábor, Jámbor Éva, **Bóna Ágnes**, Ohmacht Róbert, Márk László: Endokrin neuropeptidok LC-MS vizsgálata, Elválasztástudományi Vándorgyűlés, Tapolca, 2010.november 10-12.

Maász Gábor, Pápai Zoltán, Jámbor Éva, Petrovics Dóra, **Bóna Ágnes**, Cseharovszky Renáta, Schmidt János, Márk László: Hibernációs neuropeptidok, évszakfüggő anyagcsere változások tömegspektrometriás vizsgálata, Peptidkémiai Munkabizottság Tudományos Ülése, Balatonszemes, 2013.05. 31.

**Bóna Ágnes**, Márk László: A tömegspektrometria alkalmazása a paleopatológiában. 16. Labortechnika kiállítás, Tömegspektrometriai szakmai nap, SYMA Sport- és Rendezvényközpont, 2014. március 19.